R. & M. No. 3571

MINISTRY OF TECHNOLOGY

AERONAUTICAL RESEARCH COUNCIL
REPORTS AND MEMORANDA

Low-Speed Wind-Tunnel Tests on the Effects of Tailplane and Nacelle Position on the Superstall Characteristics of Transport Aircraft

By D. J. KETTLE and D. A. KIRBY
Aerodynamics Dept., R.A.E., Farnborough

LONDON: HER MAJESTY'S STATIONERY OFFICE

1969
PRICE £1 1*s.* 6*d.* NET

Low-Speed Wind-Tunnel Tests on the Effects of Tailplane and Nacelle Position on the Superstall Characteristics of Transport Aircraft

By D. J. KETTLE and D. A. KIRBY

Aerodynamics Dept., R.A.E., Farnborough

Reports and Memoranda No. 3571*
August, 1967

Summary.

Measurements of lift, drag and pitching moment have been made on several model configurations for wing incidences up to 53°. Tailplane and nacelle size and position were varied independently and the results confirmed that aircraft with engines mounted at the rear of the body and a high-tailplane position face severe superstall problems. For such layouts deep penetration of the stall could lead to a stable trimmed condition at a high incidence where the tailplane is in the wake of the wing and nacelles and is incapable of ensuring a recovery to normal flying attitudes. The advantage of using low-tailplane positions and of increasing the tail arm to allay the superstall problem was clearly demonstrated by the tests. Several other trends which it is considered will be of guidance to the future designer were also noted; but because of the complexity of the flow at the tailplane it is recommended that the wind-tunnel programmes on all future layouts should include some tests at very high incidence.

CONTENTS

Section.

*Replaces R.A.E. Tech. Report No. 67 197 (A.R.C. 29 746).

CONTENTS—*continued*

---

1. *Introduction.*

From many aspects, such as passenger comfort, effect of tailplane position on cruise performance, optimisation of the fin-tailplane structure, the adoption of the high-tailplane rear-engined layout for transport aircraft has its merits. At low speeds, other advantages such as the reduced susceptibility of the tailplane to changes in environment as the aircraft nears the ground, and gains in fin effectiveness are worthwhile. However, the accident to the BAC 111 in October 1963 and difficulties encountered on

other aircraft during flight proving of their stalling characteristics exposed some lack of knowledge of the aerodynamics and appreciation of the importance of the very high incidence or 'superstall' region* for T-tail configurations; previous superstall work having been confined to the low aspect-ratio fighter aircraft, Javelin and Swift, several years ago[1]. Typically the primary cause of a superstall excursion is the sudden loss of lift at the stall leading to an increase of incidence because of the increment of vertical velocity component. This rapid incidence build-up is accompanied by large increases of drag which reduce the flying speed and further increase the rate of sink. If the high-incidence characteristics of the aircraft are such that a stable trimmed condition accompanied by a loss of control power can be reached at very high incidence, an irrecoverable situation can arise.

Following the BAC 111 crash, firms' tests on a model of the aircraft in the Weybridge 13ft × 9ft tunnel and in the Farnborough 24ft diameter tunnel[2] showed that with increasing incidence beyond the stall the high tailplane passed successively through the extensive regions of low dynamic pressure associated with the wing and nacelle wakes and as a result experienced a loss of effectiveness over a very large range of incidence. The tests confirmed that at high incidence the maximum available tailplane contribution to pitching moment was so reduced, that, if the aircraft was stalled with its centre of gravity in the furthest aft position it could reach a stable trimmed point at very high incidence from which recovery could not be effected by means of the longitudinal flying controls alone.

Naturally the stability and control of an aircraft at high incidence will be influenced by the relative positions of the tailplane, nacelles and wing, and the experimental investigation described in this Report was made to determine the effects of the various aircraft components on the longitudinal stability and control of transport aircraft configurations in the superstall region. The model used was based initially on the BAC 111 dimensions but several tailplane and nacelle positions appropriate to other transport aircraft were tested, and in some cases a wide range of tailplane angle was covered so that an attempt could be made to separate the effects of reduced dynamic head from the wing and nacelle wakes and of tailplane stalling. The extent of the wing and nacelle wakes was varied by changes in wing planform and nacelle size and span. Further variations of the relative sizes of wake and tailplane were obtained by increasing the tailplane span.

In the Report the effects of changing the more important geometric parameters are discussed in detail and the results show certain trends which it is considered will be of guidance in the early stages of future aircraft design. Clearly on one basic model it was not practicable to cover every possible type of aircraft configuration and for a particular aircraft the precise superstall behaviour is so dependent on the configuration chosen that it is essential that wind tunnel programmes on new layouts should include tests beyond the stall so that the probabilities of deep-stall penetration and recovery can be assessed.

2. *Description of Model.*

The model was based largely on the BAC 111 design, to a scale of 1/15·5, which was chosen to restrict wing area/tunnel cross-sectional area ratio to the order of 0·05 so that the wake blockage corrections were minimized. A flat plate with a radiused leading edge and a chamfered trailing edge was used to represent the wing; this was considered justifiable since the programme was concerned with behaviour at high incidence where the wing was completely stalled and also had the advantage that the wing could be easily modified or replaced by alternative planforms. Fig. 1 shows the basic wing with BAC 111 planform (Model 1) and a modification to the wing root to give greater sweepback and chord (referred to as Model 2). An alternative wing (Model 3) having larger overall sweepback and span, corresponding to a modified Trident planform is shown in Fig. 2. All three wings were set low on the body at a wing body angle of 2·6°.

One further variant in the model series was provided by setting the wing of Model 1 high on the body as shown in Fig. 3; in this case the wing-body angle was 0° and the arrangement is referred to as Model 4. The majority of the tests were made with Models 1 and 2, wing span remaining unaltered, changes to the tips being considered for this investigation at high incidence to have far less effect at the tailplane than wing root modifications.

*Otherwise termed 'deep' or 'stable' stall region.

The basic body of circular cross section was similar to that of the BAC 111 except that the rear fuselage was extended slightly to permit a greater area for nacelle movement; the nose was simplified by omitting the cabin details. Forward extensions to the body were added when the larger wings were tested, to represent more balanced aircraft designs.

Two tailplanes, 1 and 2, were made (*see* Fig. 1), the first representing that of the BAC 111; the second was derived by extending the leading and trailing edges to give 20 per cent greater span (approximately 14 per cent greater area). Both tailplanes had the same symmetrical section (NACA 0010) rather than a flat plate section so as to give, as near as possible, fully representative tailplane contributions to pitching moments. Elevator controls were not represented but provision was made for varying tailplane angle over a wide range of settings (± 40 deg); tailplane geometric settings, η_B, are quoted relative to the body centreline. The model was provided with a large flatplate fin so that the same tailplane could be used for a wide range of vertical and longitudinal positions relative to the wing (Fig. 1).

Two sets of nacelles, each of circular cross section, were made. The first set, appropriate to the BAC 111 in size and shape, was tested in a number of positions (1 to 5) on the rear body. For positions 2, 3 and 4 the overall nacelle/tailplane span ratio was held constant. Position 1 represented the angled position of the BAC 111 and position 5 was intended to simulate the large overall nacelle span of a four-engined layout but still only using two nacelles (Fig. 1). The second and larger set of nacelles was matched in size and position to the larger aircraft layout of Model 3 and tested mainly with that configuration; two spanwise positions of these nacelles were tested as shown in Fig. 2, the small and large span positions being referred to as positions 6 and 7 respectively. Stub flat-plate wings filled the space between the smaller nacelles and the body, but for both spanwise positions the corresponding space with the larger nacelles was filled by more representative fairings having a 10 per cent thick aerofoil section. In order to obtain a direct comparison of the small and large nacelles, the latter were also tested in position 8 with the nacelle intakes in the same fore and aft position on the body as those of the smaller nacelles in position 1. For this test the space between nacelles and body was filled with stub flat-plate wings.

Both sets of nacelles had correct intake lip fairings leading to a constant diameter internal bore, but no attempt was made to control the intake airflow after it had been established that blocking the nacelles had a negligible effect on the overall forces and moments.

The model was not tested with wing flaps except in one case when a flat plate extension to the wing trailing edge was fitted, to simulate the increased wing chord apposite to an extending flap (Fig. 4). It was not thought worthwhile to represent all the fine details of nacelles, extending flap supports, fin/tailplane and wing/body junctions etc. since their effects, even though present at all incidences, were considered to be secondary to the main investigation. Geometric details of the models are given in Table 1, and the main geometric features in terms of wing root chord* are given in Table 2 using the notation shown in the following sketches.

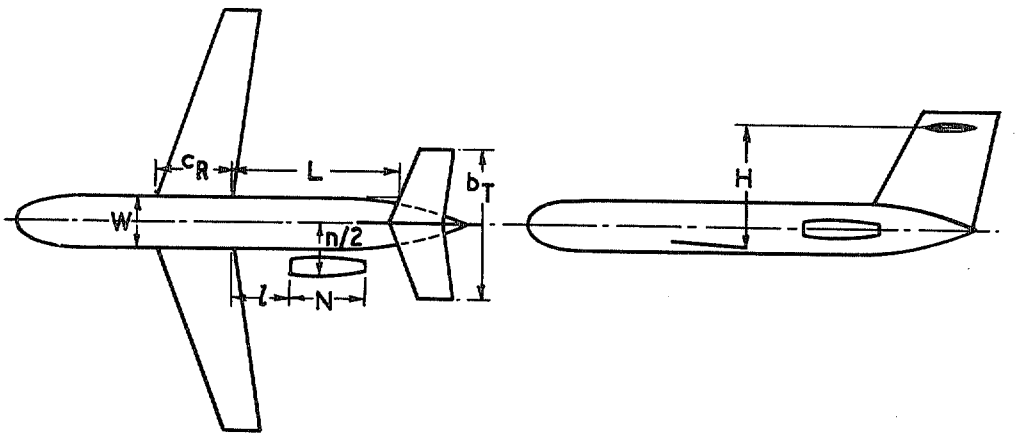

*The wing root chord c_R is defined as the wing chord at the intersection of the wing with the maximum body width in a plan view.

The range of parameters summarised in Table 2 were chosen to be representative of current transport aircraft with rear-mounted engines and T-tails and to a first order, define the relative positions of tailplane, nacelles and wing. Comparative dimensions of several transport aircraft, used as a basis for the model design, are given in Table 3 using the same notation as above. All the aircraft listed have rear mounted engines except for the HS 681; all have tailplanes mounted on the fin.

Comparing Table 3 with Table 2 which gives the details of the models, shows that for most of the parameters the model configurations covered the practical variations adequately, but the large change in the body width to wing chord ratio from 0·38 (VC 10) to 0·68 (BAC 111) was not represented. At the time of planning the test programme it was considered that in assessing the effectiveness of the tailplane, representation of the wake behind the superstalled wing was primarily related to wing chord and sweepback at the root and that the width of the body was a secondary variable. A study of the factors contributing to post-stall longitudinal stability has also been made in the U.S.A.[3] and included a moderate body-width variation. These results showed that the tailplane contribution was virtually unaffected by body width; but there could still be important effects arising from large changes in body size and cross-section.

The fore and aft position of the tailplane has been defined arbitrarily as the distance between the wing trailing edge and tailplane leading edge at the spanwise station corresponding with c_R. Table 3 shows that, in terms of c_R, the DC 9 tailplane is almost twice as far aft as that of the VC 10 comparing extreme values. Excepting the DC 9, the other aircraft have values of L/c_R in the lower half of the range (from 1·21 to 1·74). The height of the tailplane has been defined, again arbitrarily, as the distance above the wing root trailing edge measured perpendicularly to the body datum. Comparing the extreme values, the DC 9 tailplane is about twice as high as the lowest (Caravelle) but ignoring the latter case, the spread of H/c_R is within 0·5.

The tabulated values relating to the nacelles show the variations in nacelle length (excluding support fairings), fore and aft position on the rear body and overall span in terms of c_R. In all cases the values of N/c_R, l/c_R and n/c_R have a spread within about 0·5. The model nacelle sizes and locations were chosen to be representative of most of the aircraft listed in Table 3. The final row of figures in the Table gives the nacelle overall span in terms of tailplane span and for twin nacelles, the values of n/b_T are between 0·54 and 0·74; the four-engined VC 10 has a value of 0·85. No attempt was made in the model tests, to simulate the third, centrally mounted engine of the HS 121 and Boeing 727, since its effect was expected to be small compared with that of the side-mounted engines at the rear of the body.

It should be emphasised that the tests were not intended to yield accurate information on the high-incidence stability characteristics of the specific aircraft listed in Table 3. Precise data of this kind can only be obtained using scale models with fully representative details.

3. *Details of Tests.*

The model was supported by means of struts attached to the balance frame and pivoted about a pitching axis by means of cleats fixed to the wing. A single pitch wire to control model incidence was attached to the pitching-moment balance. Three-component measurements (lift, drag and pitching moment) were made over an incidence range up to about 50° and the results have been corrected for tunnel constraint and wake blockage effects[4]. The latter correction to dynamic head depends on the relative size of model and tunnel. In the present experiment the correction increased almost linearly with model incidence stability characteristics of the specific aircraft listed in Table 3. Precise data of this kind can only it amounted to an increase of dynamic head of about 20 per cent for the largest model configuration and about 12 per cent for the smallest.

Initially it was assumed that a length of 20 swg wire attached round the body about $7\frac{1}{2}$ inches aft of the nose would be sufficient to fix transition on the body, but the early test results showed, at incidences above about 30°, evidence of laminar flow separations occurring in the cross flow on the body aft of the nose wire. The extent of the laminar flow varied with the distance between the nose wire and the wing. The pitching moment results in particular showed that there was a need to standardize the fuselage

cross-flow separations and it was necessary to fix two additional lengths of 20 swg wire to the sides of the body, parallel to the axis. The wires were lengthened when the fore-body overhang was increased as with Models 2 and 3.

Table 4 summarises the range of model test configurations made in the No. 1 $11\frac{1}{2}$ft × $8\frac{1}{2}$ft tunnel at the R.A.E. Farnborough at intervals during 1964 and 1965; a nominal tunnel speed of 120 ft/sec was used throughout the investigation.

4. *Presentation of Results.*

4.1. *General.*

Since the investigation was concerned with longitudinal pitching behaviour up to high incidences, the results are presented mainly as curves of pitching-moment coefficient (C_m) against wing incidence (α_w). Some curves of lift coefficient (C_L) and drag coefficient (C_D) against wing incidence have been included and the force coefficients have been used to analyse the tailplane contributions to pitching moment. The analysis, given at the end of the Report, while not providing a complete understanding of the flow conditions near the tailplane, has helped to explain the pitching characteristics in the moderate to high incidence range; photographs of tufts on the upper surface of the tailplane in certain basic configurations of the model, are included and confirm some of the conclusions reached.

4.2. *Pitching-Moment Results.*

The analysis of pitching-moment results on a range of model configurations, (e.g. varying tail size and arm) emphasized the need for a basis for comparing the results. The pivot axis chosen for the basic wing (Model 1) was at $0{\cdot}41\bar{c}$ corresponding with the aft cg limit on the BAC 111. The wing of Model 2 obtained by a forward extension of the chord over the inboard sections, used the same pivot axis relative to the trailing edge, resulting in a moment-centre position at about $0{\cdot}63$ of the modified $\bar{c}$. This represented an unrealistic location leading to basically unstable pitching moments and when analysing the results it was therefore necessary to shift the moment centre forward. Similarly, shifts of moment-centre position were made with Models 3 and 4 and when tail size or arm was changed. The method adopted in all cases, was to adjust the moment centre to give the same dC_m/dC_L at low incidence as for the basic model configuration (Model 1 with tailplane 1 in B2 position). In general, the addition or movement of nacelles resulted in a negligible shift of aerodynamic centre at low incidence and so the moment centres for the corresponding no nacelle cases were retained. To avoid possible confusion from the use of different reference moment centres, the curves of pitching moment have been annotated to indicate the moment centre or cg used. For convenience the moment centre is referred to hereinafter as a cg position. In some cases, the results are quoted with and without modification to cg position so that the effect may be seen.

5. *Preliminary Results.*

5.1. *Description of Stall Development on Flat-Plate Wing.*

Before proceeding to the discussion of the main results, a brief description of the flow over the wing is necessary particularly since a flat plate was used. Short tufts were taped to the upper surface of the wing and visual observations made of the stall development on wings of Models 1 and 2. In general, the flows on the two wings were the same, the only difference being that the root sections stalled at a higher incidence on Model 2 and this was probably related to the reduction in local lift coefficient with the increased root chord of Model 2. The observations on Model 1 showed that, as would be expected, separations developed first at the leading edge over the outer semi-span at an incidence of about $2\frac{1}{2}°$. By about 6° the outer 30 per cent of the span was completely stalled and as incidence was increased the stall moved inboard until at about 10° the outer 90 per cent of the net span was stalled; between 10° and 11° the remaining 10 per cent inboard stalled. The inboard development of the stall on Model 2 was slower and it was not until about 17° of incidence that the whole wing was completely stalled.

A true sectioned wing would not be expected to begin to stall at the low incidences found on the flat-plate models and the wing would not be completely stalled until much later (nearer 20° of incidence), so the wing wake is unrepresentative on the flat-plate models for most of the incidence range below $\alpha_w = 20°$; the extent to which the results might be invalidated in this region is discussed in the following Section.

5.2. *Comparison with Fully Representative Model Tests.*

Data from 24ft wind-tunnel tests[2] on a fully representative 1/10 scale model of the BAC 111 are compared with that obtained on the present model (BAC 111 configuration) for the same tailplane setting in Fig. 5. Analysis of a similar comparison made for the models without tailplanes showed that about one third of the difference in model pitching moment recorded at low incidence must arise from the lack of representation of the fine detail of the extending flap supports, wing-body junctions etc. on the research model. Incorrect fin representation and the different fin-tailplane junctions probably accounts for the remainder of the discrepancy. At higher incidences differences in tail load resulting from junction effects will be reduced because of the reduction in stream dynamic head behind the wing and it is noticeable that above the stall the C_m curves in Fig. 5 run together. This figure shows that the results for the two models are so similar and show the same trends as incidence is increased that except for the incidence range $\alpha_w = 8$ to 20°, where the wing is stalling, the important features of the wing and nacelle wake are reproduced on the flat-plate model in sufficient detail to give confidence that the main effects of varying tailplane and nacelle position could be ascertained reliably on the simple model.

The curves for the 1/10 scale model in Fig. 5 illustrate the adverse pitching-moment characteristics of the BAC 111 in the 'superstall' region. Above an incidence of about 20°, the pitching moments show longitudinal instability and reach a maximum positive value at about $\alpha_w = 45°$. At higher incidences the curve has a stable slope with a trimmed incidence in excess of 50°. It will be shown later that the control power available at high incidences falls to a very low value because of the large loss of dynamic head at the tailplane. Recovery from a stable trimmed attitude at high incidence is thus rendered difficult and is improbable with the normal longitudinal trimming controls if the tailplane and elevator are unable to supply a nose-down moment throughout the post-stall region. This is often the case with T-tailed aircraft flying at their aft cg positions and it will be seen in the following results that many of the rear-engined configurations tested exhibited pitching moment-characteristics similar to those shown in Fig. 5 differing only in the extent and severity of the pitch-up region.

6. *Results without Nacelles.*

6.1. *Comparison of Models.*

6.1.1. *Lift.* The variation of lift coefficient with incidence is shown in Figs. 6, 7 and 8. Fig. 6 compares the results for the Models 1 to 4 without nacelles and tailplane and the curves support the observations of Section 5.1 that the wing of Model 2 was not completely stalled until an incidence greater than the corresponding value for the wing of Model 1. Model 3 shows similar results to Model 2 except that the values of C_L for Model 3 are noticeably higher at the higher incidences where the effect of the longer forebody is most marked*. The differences in C_L between Models 1 and 4 must arise mainly from the change in wing height since there was no difference in overall body length and only a small change in forebody length (*see* Figs. 1 and 3). The curves for all the models show that even when there is complete breakdown of the flow over the wing the lift continues to rise slowly with incidence up to values of α_w of about 40°.

Modern transport aircraft, particularly those with rear-engined configurations, need large tailplane areas in order to be able to trim the aircraft in low-speed flight with high-lift devices in operation. The effect on lift of a typical tailplane (area of the order of 25 per cent of the wing area) is demonstrated by the results from tests with tailplane 1 in position B2 plotted in Figs. 7 and 8 for Models 1 and 2 re-

*As will be seen later in Section 6.2 the increase in lift on the forebody when the forebody length is increased has a large effect on the pitching moment.

spectively. The curves show the extent of the tailplane contribution to the overall lift through the incidence range and indicate the conditions in which the wing wake and/or tailplane stalling reduce the tailplane lift.

6.1.2. *Drag.* The drag coefficients plotted in Figs. 9 and 10 for Models 1 and 2 respectively show the rapid increase of drag with incidence, values of C_D in excess of 1·0 being reached at $\alpha_w = 50°$. The contribution of the tailplane to model drag is very dependent on the local flow direction at the tailplane since when the tailplane is at only a moderate incidence to the local flow the tailplane lift rather than its drag can be the more important source of overall drag increases. The predominate features of the flow at the tailplane positions are discussed later in Section 9; the analysis confirms that the tailplane drag has a relatively small influence on the overall forces and moments acting on the model except when the tailplane is stalled. The results shown in Figs. 9 and 10 are typical of all the model configurations tested.

6.1.3. *Pitching moments.* Figs. 11, 12, 13 and 14 show the variation of pitching-moment coefficient with incidence for Models 1, 2, 3 and 4 for the smaller tailplane in the B2 position. At this location, the tailplane was at the same height above the wing trailing edge for models 1 to 3 but for Model 4 the height above the wing was halved due to the high wing position. Extensive regions of longitudinal instability for Models 1, 2 and 3 are evident in the medium incidence range. At these attitudes the tailplane is immersed in the wake from the wing, a region of increased downwash and reduced dynamic head as shown later in the Report. Eventually the tailplane emerges below the wing wake and at incidences above about 35° the pitching-moment curves have a stable slope; depending on the tail setting, a high trimmed incidence is reached which may be in excess of 50° as for example with Model 3. These adverse pitching-moment characteristics are shown in Section 6.3 to be dependent on tailplane height above the wing and the results for Model 4 (Fig. 14) show that when the tailplane is sufficiently low relative to the wing, longitudinal instability does not occur except to a small extent in the low incidence range where the present tests on a flat-plate wing are unrepresentative.

The curves of Figs. 11 to 14 also show the changes of C_m with tail setting. With increasing incidence there is a reduction in control power ($\partial C_m/\partial \eta_B$) which occurs because of the combined or separate effects of tailplane stalling and loss of dynamic head at the tailplane. Attempts have been made in the analysis of Section 9 to disentangle these two effects but with limited success; and it is clear that when the tailplane is immersed in the wing wake at high incidence, its value as a trimming device is seriously affected. This result is not surprising considering the nature of the flow within the separation 'bubble' behind the wing where even reversal may occur[1]. Tuft observations on the tailplane upper surface during the course of the present experiments confirmed this.

Later results described in Section 7, show evidence that nacelles at the rear of the body add their own wakes to that of the wing and at the same time cause an increase of downwash at the tailplane (*see* Section 9) thus reducing the effective tailplane incidence. The results emphasize the complex nature of the flow at the tailplane and the need for wake surveys.

6.2. *Effect of Forward Extension to the Body.*

Extension to the wing chord over the inboard sections was accompanied in all cases by a forward extension to the body (Model 2). The effect of extending the body alone was investigated in a separate test using Model 1 and tailplane 1. The results are shown in Fig. 15 with and without tailplane (position B2) and increased pitch-up trends due to the extended body are apparent, even when the cg location is moved forward to compensate for the destabilising effect at low incidence. The tailplane contributions to pitching moments however, appear to be little affected by the increased length of body at the nose, suggesting correspondingly small alterations to flow conditions at the tailplane. Similar conclusions were reached in Ref. 3 for moderate increases in cross-section size as well as for increases in forebody length.

6.3. *Effect of Tailplane Height.*

The influence of tailplane height above the wing on the pitching-moment characteristics of Models 1, 2 and 4 is shown in Figs. 16, 17 and 18 respectively. The results for Model 4 show an almost complete absence of pitch-up tendencies for all of the tailplane positions tested. This is to be expected since the

corresponding tailplane positions are relatively closer to the wing in the high-wing configuration and at high incidence are all immersed in a region of lower downwash compared with the low wing arrangement. However, it is anticipated that the high wing configuration would exhibit unstable characteristics post-stall, if the tailplane were set sufficiently high relative to the wing, i.e. higher than position B1.

For the low-wing Models 1 and 2 the adverse effect of increasing tailplane height on the pitching moments is demonstrated clearly in Figs. 16 and 17, the pitch-up region extending to about 40° of wing incidence for position B1. This region will be shown later in the Report to be caused initially by non-linear variations of downwash with incidence and aggravated by loss of dynamic head at the tailplane. Eventually the tailplane emerges below the field of downwash and low dynamic head at an incidence dependent on tailplane height, leading to a region of high incidence stability. Furthermore, a stable, trimmed incidence is reached (44° for tailplane position B1 and 38° for B2) where there may not be sufficient control power to effect recovery. The results clearly demonstrate the advantages of low tailplane positions in avoiding a recovery problem post-stall, the curves for position B4 for example, showing no pitch-up relative to the extension of the low incidence C_m vs. α_w line. Undue significance should not be given to the low incidence instability found on Model 2 with low tailplane since it occurs in the incidence range where the flat plate wing is known to be unrepresentative.

6.4. *Effect of Tail Arm.*

The influence of tail arm on the post-stall pitching-moment characteristics is shown in Fig. 19 for Model 1; the beneficial effect of the aft tail position (D2) is clearly demonstrated. The results are given for a cg position at $0{\cdot}41\bar{c}$ and show similar large effects to those due to variation of tail height described in the previous Section. Position D2 produces an unstable region from $\alpha_w = 20°$ to 28° but a stable trimmed incidence is not reached as with the further forward tail positions. At the same time, the stability margin defined at low incidence is increased by the larger tail arm. Assuming this can be tolerated from trim and stick forces/g aspects, the result for D2 suggests there is no superstall problem as with positions A2 and B2.

If, on the other hand, the cg locations for tail positions A2 and D2 are adjusted to give the same low incidence stability margin as for B2* the degree of pitch-up for A2 is reduced and that for D2 is increased. The adjusted pitching-moment curves are compared in Fig. 20 and although the relative merits of the extreme fore and aft tail positions are not significantly affected, the result for D2 is nearer to indicating superstall difficulties with the further aft cg position ($0{\cdot}5\bar{c}$). The results presented emphasize the advantages of a larger tail arm in easing the superstall problem provided the low incidence static margin does not require to be reduced excessively by aft movements of the cg. Tailplane geometry could also be a dominant parameter in this respect and is discussed in the following section.

6.5. *Effect of Tail Size.*

All the results described so far were obtained with tailplane 1 which, in position B2 corresponded with that of the BAC 111. Results for tailplanes 1 and 2** are compared in Fig. 21 where it is seen that the extra span causes a nose down moment (referred to the same cg at $0{\cdot}41\bar{c}$) which is roughly constant over the incidence range from 20° to 50°. The larger tailplane appears to effect an improvement at high incidence but at the expense of a larger static margin at low incidence as would be expected. If the curve for tailplane 2 is adjusted to give the same margin at low incidence as for tailplane 1, most of the high incidence advantage is lost; a stable trimmed attitude is reached just below 40° and the result is almost identical to that for the smaller tailplane.

The results discussed in the preceding paragraphs have emphasized the sensitivity of pitching moments to tailplane location on the fin where large variations in downwash are known to occur. It follows that changes to tailplane geometry (e.g. sweepback and/or taper ratio) would exert an influence on the overall

*The choice of stability margin at low incidence is arbitrary in this context, but the superstall characteristics are obviously affected at the same time. The aft cg position on particular configurations may therefore require to be fixed with both pre-stall and post-stall stability characteristics in mind.

**20 per cent increase of span, 14 per cent increase of area compared with tailplane 1.

pitching moments at high incidence. For example, a tailplane having greater sweepback might be expected to have a beneficial effect on the high incidence behaviour by virtue of its tips being immersed in a reduced field of downwash.

7. *Results with Nacelles.*

7.1. *Comparison of Models* 1, 2 *and* 3.

Typical sets of curves for complete model configurations are shown in Figs. 22, 23 and 24 for Models 1, 2 and 3, the first two with small nacelles and the latter with the larger nacelles appropriate to that wing-body configuration. The results for Models 2 and 3 have been adjusted to have the same static stability at low incidence as for Model 1. Comparing the curves for $\eta_B = 0°$, unstable trends above $\alpha_w = 20°$ are evident for each configuration. Compared with the no nacelle results (Figs. 11, 12 and 13) the incidence range over which instability occurs is seen to be extended at the higher end. For Models 1 and 2, stable pitching moments are reached at an incidence of about 46° and for Model 3 the stable region has not been reached by 53°. The results demonstrate that the tailplane has to pass through the wake and downwash influence of the nacelles, additional to that of the wing, so rendering it ineffective over a larger incidence range. The stable region is reached only when the trailing edge of the tailplane begins to emerge below the wake from the rear of the nacelles; the incidence at which this occurs is related to the fore and aft position of the nacelles on the body and the height of the tailplane above the nacelles. It follows that the further aft position of the nacelles on Model 3 (Fig. 24) compared with the smaller nacelles of Model 1 (Fig. 22) is reflected in a more extensive region of pitch-up. From Fig. 24 it may be inferred also that when nacelles are located very far aft on the body the wakes from wing and nacelles may be isolated from each other, leading to two distinct regions of pitch-up as the tailplane passes through each wake in turn.

The effects of nacelle position and size on the overall pitching-moment characteristics are discussed in more detail below. Figs. 22, 23 and 24 when compared with Figs. 11, 12 and 13 indicate that the nacelles amplify the loss in control effectiveness at high incidence and this aspect is discussed further in Section 8.

7.2. *Effect of Fore and Aft Location of Nacelles.*

The effect of fore and aft location of the small nacelles, without tailplane, is shown in Figs. 25 and 26 for Models 1 and 2 respectively. For both wing planforms the addition of nacelles causes a negative change of pitching moment which increases rapidly with angle of incidence above $\alpha_w = 20°$ at a rate dependent on the fore and aft position of the nacelles. Since the moment change is governed by the point of action of the nacelle lift the nacelles are progressively stabilizing as their distance behind the pitch axis is increased. In the presence of the tailplane, however, the nacelle effects on pitching moment are less straightforward because of the influence of the nacelle wake. For the tailplane in the B2 position Figs. 25 and 26 show that the presence of the nacelles extends the region of pitch-up by an amount which depends on their fore and aft location. The pitch-up region is prolonged more for the aft nacelle position; in the forward position, pitch-up extends only as far as $\alpha_w = 40°$ but the maximum positive pitching-moment coefficient realised is considerably larger. For all positions tested, the pitching moments with nacelles are more positive above an incidence of about 40° because of increased downwash at the tailplane. On this evidence it is doubtful whether the pitch behaviour at high incidence can be substantially improved for T-tail configurations, solely by longitudinal positioning of nacelles.

The effect of nacelle position in conjunction with changes in tailplane size is shown in Fig. 27; increase of tailplane span does not materially affect the results comparing fore and aft nacelle location. The comparisons are given for a cg position at $0{\cdot}41\bar{c}$ and demonstrate the stabilizing effect of the larger tailplane. Assuming that adjustment to cg position with tailplane 2 is required to maintain the same low incidence stability margin as for tailplane 1, the beneficial effect of the larger tailplane would be lost at high incidence, supporting the conclusions reached in Section 6.5 without nacelles. A further feature of the results given in Fig. 27 is that the differences between the curves for nacelle positions 1 and 3 are small as would be expected.

7.3. *Effect of Vertical Location of Nacelles.*

The effect of vertical location of the small nacelles at longitudinal position 3 with tailplane 1 in the

B2 position is shown in Fig. 28; below an incidence of about 40° the pitching moments are little affected. At higher incidences the pitch-up region is extended slightly by lowering the nacelle position $1\frac{1}{2}$ inches model scale and this result is consistent with the tailplane emerging below the nacelle wake at a higher incidence. The severity of pitch-up is the same as for the high nacelle position.

One further nacelle arrangement was tested with tailplane 1 in the B2 position, in which the nacelles were positioned on the top shoulder of the body, 30° from the model plane of symmetry and at the same fore and aft location as position 3. This position had been shown in some small scale tuft experiments by Gray[5] to have negligible effect on the downwash at the tailplane; tests on Model 1 confirmed that the severity and extent of the pitch-up region was reduced to the level obtained without nacelles (Fig. 28) i.e. still showing a stable trimmed incidence of about 38°. It is doubtful whether such moderate improvement in the pitching moment characteristics is sufficient to prevent deep-stall penetration and in addition there would be practical problems of installation with this high nacelle position.

7.4. *Effect of Nacelle Size and Span.*

The majority of the tests were made with the smaller nacelles corresponding to those on the BAC 111; larger nacelles were tested mainly with Model 3 but in order to determine the effect of nacelle size on the pitching-moment characteristics, a separate test was made using the larger nacelles in conjunction with Model 1. In addition, tests were made to investigate the effect of nacelle span with both the small and large nacelles. For this purpose, the overall span of the smaller nacelles was increased by about 25 per cent on Model 2 and that of the larger nacelles by about 10 per cent on Model 3; in each case, the increase was achieved by means of a wider nacelle/body fairing. The results are illustrated in Fig. 29.

The effect of nacelle size on Model 1 is shown in Fig. 29a; the pitching moments are not affected below an incidence of about 26°. At higher incidences the results show that the positive values of C_m reached are smaller with the large nacelles, suggesting a modified nacelle wake. In the absence of elaborate wake surveys it is not possible to say to what extent this is due either to changes of downwash or dynamic head at the tailplane with the larger nacelles. Nacelle span effects were also found at high incidence (*see* Figs. 29b and c) though they were of smaller magnitude than those due to nacelle size. The limited number of nacelle configurations tested show that large variations may occur in the high incidence pitching-moment characteristics and for this reason model tests on particular layouts in the 'superstall' region are considered an essential requirement.

7.5. *Results with Alternative Tailplane Positions.*

A number of alternative tailplane positions were tested on Models 1 and 2 with nacelles in positions 3 and 4 respectively; the range of model configurations was not so extensive as those described in Section 6 and so presentation of systematic results is not possible. Some of the more significant results are summarized in Figs. 30 and 31.

Fig. 30 compares the B2, D1 and D2 positions of tailplane 1 on Model 1 and the cg has been adjusted for the D positions to compensate for the increased tail arm. The rear tail position D2 shows to advantage compared with B2, the severity and extent of the pitch-up region being reduced. The important differences between this result and that obtained without nacelles (Fig. 20) is that in the present case there are positive pitching moments above 30° with a stable trimmed incidence at 45°. These features are paramount in contributing to 'superstall' difficulties. The curves of Fig. 30 suggest that if the tail arm were sufficiently large, i.e. greater than that for D2, the pitching-moment characteristics might be made acceptable by the avoidance of positive pitching moments entirely at high incidence. Further tests would be needed to substantiate these suggestions.

The adverse effect of raising the tailplane position from D2 to D1 is clearly shown in Fig. 30 confirming the general conclusion of Section 6.3 that increase of tailplane height above the wing has a detrimental effect on the pitching-moment characteristics. The advantage of the low tailplane combined with that of an aft position (C3) on Model 2 with the small nacelles in position 4 is demonstrated in Fig. 31. With this configuration there is little evidence of pitch-up except at incidences below 20° where the results are known to be unrepresentative.

7.6. *Results with Flaps.*

Deflected slotted flaps were not considered practical with a flat-plate wing and so it has not been possible to investigate their effect with the present model. One test was made however with a flat-plate extension to the trailing edge of the wing of Model 1 to give a simple representation of extended flaps without deflection. With this arrangement it was hoped that the wider wake would simulate as far as possible the separated flow behind a correctly sectioned wing with slotted flaps. In general the results with flaps are typical of most of those previously described, in showing pitch-up trends from about $\alpha = 20°$ to 40°, followed by a stable region with a trimmed incidence in excess of 50°. There are no major effects due to flaps as tested but there is a need for further investigation at high incidences on a model with true wing and flap section details. Particularly, it is necessary to determine the flow conditions at the tailplane with slotted flaps in the deflected position.

8. *Tailplane Effectiveness.*

The pitching-moment coefficients plotted in Figs. 11 to 13 and 22 to 24 show that for high-tailplane configurations the ability of the tailplane to control such aircraft beyond the stall is poor, and in some cases the tailplane effectiveness decreases so rapidly with incidence that recovery from a trimmed state at high incidence may be impossible. This loss of control power is due mainly to the reduced dynamic head in the wake from the wing and nacelles, but the experimental evidence is confused in certain cases by the additional effect of stalling of the tailplane. Attempts to disentangle the two effects at high incidence have proved to be difficult – *see* Section 9. Within the practical range of tailplane movement (or combined tailplane and elevator movement) the increment in C_m due to $\Delta\eta_B = -10°$ can conveniently be used as a measure of the tailplane effectiveness and this increment, non-dimensionalized relative to the values of C_m for $\Delta\eta_B = -10°$ at low wing incidences, is plotted in Figs. 33, 34 and 35 for several model arrangements. Because of the complex nature of the flow at the tailplane no elaborate analysis of the results can be made but certain trends are apparent and are discussed below.

Without nacelles the curves show that in the medium incidence range tailplane effectiveness is slightly improved when the tailplane is set low on the fin (B4 position in Fig. 33a); similarly the rearmost tailplane position (D2 in Fig. 33b) appears to be marginally better than the forward positions. At incidences above 50° all tail positions show values of ΔC_m which are about 1/5 of the normal low incidence value, due in part to tailplane stalling. The extent to which dynamic head might have recovered in this region is conjectural and requires to be confirmed by wake traverse measurements.

The results with nacelles (Fig. 35) show that in the incidence range above 40°, further losses of control effectiveness occur except in one instance when the small nacelles are mounted in a forward position close to the wing. For this arrangement, extra downwash due to nacelles may partially inhibit tailplane stalling as discussed in Section 9, but more direct evidence from wake surveys is required to confirm the downwash and dynamic head pattern in this region. The effect of increasing either nacelle size or span is shown to cause only a small loss of tailplane effectiveness for incidences above about 40° (Fig. 35) but above 50° it is as low as 1/10 of the normal value. Thus, for large nacelle installations towards the rear of the fuselage, recovery from high, stable trimmed incidences with conventional pitch controls will be difficult if not impossible.

9. *Analysis of Tailplane Contribution to Pitching Moments.*

The pitching-moment results presented in this Report have shown that the high incidence behaviour of an aircraft is critically dependent on the position of its tailplane. Re-location of the tailplane could lessen and in some cases avoid the superstall problem. In order to obtain a better understanding of the role of the tailplane at high incidence and its contribution to the pitching moments it is necessary to determine the flow environment in the tail region. In the absence of detailed wake measurements an attempt has been made to identify the predominant features of the flow at the tailplane by an analysis of the forces acting on the tailplane. This analysis, which was confined to the basic model configuration (BAC 111) with and without nacelles assumed that the complex flow conditions at the tailplane could be replaced by mean values of the downwash and dynamic head. Details of the algebraic relationships

used are summarised in Appendix A and the derivation of the data is discussed in the following paragraphs.

(1) The average downwash ($\bar{\varepsilon}_T$) at the tailplane was determined at a number of points on the pitching-moment curves where the tailplane normal force was known to be zero, i.e. at the intersections of the curves for tail on and off and where it was assumed that the tailplane was effectively at zero incidence relative to the local flow*. The values of 'integrated' downwash determined in this way are plotted against wing incidence in Fig. 36a with and without nacelles. The most noticeable feature without nacelles is the reduction of the downwash at high incidence when the tailplane emerges below the wing wake. With nacelles, the downwash continues to rise up to wing incidences of nearly 50°. For comparison, the average downwash for tailplane 2 is shown in Fig. 37a showing in general, smaller values than for tailplane 1. Visual tuft observations without tailplane showed a variation in downwash angle decreasing with distance normal to the fin, thus supporting the evidence of the 'integrated' values obtained with the larger span tailplane.

(2) Values of effective tailplane incidence ($\bar{\alpha}_T$) were derived from the downwash and are plotted in Figs. 36b and 37b for tailplanes 1 and 2 set at $\eta_B = 0°$. Without nacelles, the reduction of downwash at high incidence results in large values of $\bar{\alpha}_T$; with nacelles the values of $\bar{\alpha}_T$ are constrained to a more moderate level due to large mean downwash angles associated with the nacelle wake. Tailplane 2 is effectively at a larger incidence due to being immersed in a smaller mean downwash field.

Surface tufts on the upper surface of tailplane 1 were photographed and show extensive areas of flow separation in the absence of nacelles (Fig. 40); with nacelles, separations are still present (Fig. 41) but the flow is relatively closer to the chordwise direction over the inboard region consistent with lower tailplane incidences derived from the estimated values of downwash (*see* patterns at $\alpha_w = 42{\cdot}6°$ with and without nacelles).

(3) The average dynamic head at the tailplane was obtained from the values of $dC_m/d\eta_B$ at zero tailplane normal force. The values of $\bar{q}_T$ expressed in terms of free stream dynamic head are shown in Fig. 36c; the curves indicate the rapid loss of dynamic head with incidence above $\alpha_w = 20°$ falling to about $0{\cdot}25\, q_0$ at $\alpha_w = 40°$. At higher incidences, $\bar{q}_T$ continues to decrease in the presence of nacelles but without nacelles, dynamic head is partially recovered. The random nature of the flow means that the analysis must be viewed tentatively in this region and for this reason the curves of effective downwash and tailplane incidence are also shown in dotted line.

(4) Tailplane lift and drag data were obtained from the overall differences of lift and drag measured on the complete model, with and without tailplane. The data were converted to orthogonal axes coincident with and normal to the mean downwash, $\bar{\varepsilon}_T$, already determined and are shown plotted against $\bar{\alpha}_T$ in Fig. 38. Both $C_{L_T}^{\bar{\varepsilon}_T}$ and $C_{D_T}^{\bar{\varepsilon}_T}$ are based on tailplane area and mean dynamic head at the tailplane, but in order to eliminate any possible uncertainties due to reduced dynamic head in the wing wake, the coefficients plotted include only those measurements at small wing incidences where $\bar{q}_T$ was close to the free-stream value. Fig. 38 shows that the points are scattered to a greater extent than would have been obtained from direct measurement of the forces on an isolated tailplane; this is due to inaccuracies inherent in the difference method of estimation and to flow unsteadiness in the tailplane flow environment.

Using the data assembled in Figs. 36 and 38 and the method given in Appendix A calculations were made of the change in pitching-moment coefficient due to tailplane assuming that the tailplane resultant force acted at the mean quarter-chord point of the tailplane at all incidences. The subsequent calculated values of C_m for the model with tailplane set at $\eta_B = 0$ are compared with measured values in Fig. 39, both with and without nacelles. The closeness of these comparisons is a measure of the degree to which the use of mean values of ε_T and q_T can be justified. With nacelles and for low incidences without nacelles the agreement is fair, but for incidences above about 30° without nacelles there is a very large discrepancy because the tailplane contribution is grossly underestimated by the method. Although this means that the values of $\bar{\varepsilon}_T$ and $\bar{q}_T$ shown for this condition ($\alpha_w > 30°$, without nacelles) in Fig. 39 are not representative of the flow at the tailplane we can assume that the local tailplane incidence is high and that at least some parts of the tailplane will be stalled. This assumption, coupled with the information presented in

*Note: the effect of the tailplane axial force is small and has been neglected and no allowance has been made for the effects of flow curvature.

Fig. 11 (where for the higher incidences the slope $\frac{\partial C_m}{\partial \eta_B}$ was less at the zero tailplane load point than elsewhere), indicates a degree of complexity in the flow which cannot be reconciled with the mean-flow concept.

The better agreement shown in Fig. 39 for the configuration with nacelles and the evidence of a more constant $\frac{\partial C_m}{\partial \eta_B}$ for this case shown in Fig. 22 implies that the flow at the tailplane is more even when the nacelles are present and the downwash is larger, i.e. the tailplane incidence is lower. To some extent this result might be fortuitous but does give confidence in using the values of $\bar{\varepsilon}_T$ and $\bar{q}_T/q_0$ to understand pitching-moment curves for the complete model. Thus the rapid increase in pitching moment beyond $\alpha_w \simeq 18°$ is shown by the analysis to be due to a relatively small increase of downwash and reduction of dynamic head with wing incidence (*see* Fig. 36). The stable region in the C_m vs. α_w curve eventually reached at high incidence occurs when the downwash is decreasing and dynamic head is being recovered.

Without nacelles it is reasonable to assume that the recovery in dynamic head at the higher incidences is larger than is shown by the analysis and the marked increase in longitudinal stability above $\alpha_w \simeq 40°$ occurs because of the increasing nose-down moment applied by a tailplane which is stalled in a comparatively high velocity flow.

It is evident that because of the complexity of the flow only a limited analysis can be made by the use of force and moment results alone. To provide a better understanding of the tailplane contribution detailed wake traverse measurements would be necessary.

10. *Modifications to Cure the Superstall.*

The tests discussed in Section 6 showed how, with low tailplane positions, pitch-up and the consequent possibility of superstall problems could be avoided. For Model 1 with tailplane 1 in the high tailplane position B2 various measures were tried during the course of the experiments in attempts to improve the pitching-moment characteristics. Flaps were fitted on the rear of the body and on the nacelle/body fairings in the hope that the adverse downwash field might be favourable influenced, but with no success.

Gray[6], in some small scale experiments, has shown that some advantage may be gained if the flow round the nacelles is controlled by a slat, but further work is required to show the effect on high-incidence pitching-moment characteristics and to assess the practicability of installing such a device.

A possible method of effecting an improvement in the pitching-moment characteristics is to induce asymmetric flow at the tailplane, so that part of the tailplane is partially cleared of the wing-body-nacelle wake and regains effectiveness. Fig. 42 shows that a considerable reduction in pitching moment was obtained by the application of sideslip. Whether or not this change in moment could be used to effect recovery of an aircraft from the superstalled state must of course depend on the dynamics of the aircraft at high incidence and the available control power when the rudder is immersed in a region of low dynamic head.

11. *Concluding Remarks.*

The results obtained in the present investigation have helped to provide an understanding of the main features of the 'superstall' problem. In general, it is confirmed that with engines positioned at the rear of the body and with the tailplane located high relative to the wing, a stable trimmed incidence in excess of 40° may be reached and in this region control power of the tailplane has fallen sufficiently so as seriously to affect the possibility of recovery. The advantages of using low tailplane positions is clearly demonstrated. Further benefit may also be obtained by increasing the tail arm, but increase of tailplane area does not show any advantage if the centre of gravity is moved to keep a constant static margin. All nacelle positions tested showed a detrimental effect except for a top shoulder position on the body, which appears to limit the extent of the pitch-up region to that obtained without nacelles.

Detailed analysis of the results with the BAC 111 configurations has shown that the tailplane contribution to pitching moments may be understood using derived data. The pitch-up characteristics occurring above about 20° of incidence are shown to be directly related to an increase of downwash

and loss of dynamic head at the tailplane. The flow conditions at the tailplane when wing incidences approach 50° could not be defined so clearly but the evidence suggested a partial recovery of dynamic head leading to a high, stable, trimmed incidence. None of the measures tried on the model was effective in controlling pitch-up tendencies with high tailplane positions but beneficial effects were found with 20° of sideslip.

The results have emphasized how the powerful effects of the downwash field behind a stalled wing have combined with low dynamic pressures at the tailplane to produce a flight condition from which recovery is difficult. It is strongly recommended that wind-tunnel model tests should be made up to high incidences on new aircraft layouts so that an assessment of the chances of entering into and recovery from a superstalled state can be made.

REFERENCES

No.	*Author(s)*	*Title, etc.*
1	D. A. Kirby and A. Spence	Low-speed tunnel model tests on the flow structure behind a delta wing aircraft and a 40° swept wing aircraft at high incidences. A.R.C. R. & M. 3078 (1955).
2	R. R. Jessop	Superstall stability tests on the BAC 111 in the R.A.E. open jet wind tunnel. Unpublished BAC Weybridge Ltd. Wind tunnel report.
3	Robert T. Taylor and Edward J. Ray	A systematic study of the factors contributing to post stall longitudinal stability of T-tail transport configurations. Presented at the AIAA Aircraft Design and Technology Meeting, Los Angeles, California (1965).
4	E. C. Maskell	A theory of the blockage effects on bluff bodies and stalled wings in a closed wind tunnel. A.R.C. R. & M. 3400 (1963).
5	W. E. Gray	Low-speed wind-tunnel tests to investigate the flow structure behind stalled wing-body combinations. Unpublished R.A.E. work.
6	W. E. Gray	Preliminary tests of a device to reduce the wake of rear nacelles on a superstalled high-tail aircraft. Unpublished R.A.E. work.

APPENDIX

Estimation of Tailplane Contribution to Pitching Moment.

The tailplane lift and drag data were obtained from differences on the complete model with and without tailplane. C_{L_T} and C_{D_T} obtained in this way were relative to measured (wind) axes.

The tailplane data presented in Fig. 38 is referred to effective incidence axes depending on mean downwash, $\bar{\varepsilon}_T$ given by

$$\bar{\alpha}_T = \alpha_B + \eta_B - \bar{\varepsilon}_T \tag{1}$$

Since

$$\alpha_B = \alpha_w - 2{\cdot}6° \text{ (wing-body angle } = 2{\cdot}6°).$$

Equation (1) becomes

$$\bar{\alpha}_T = \alpha_w - 2{\cdot}6 + \eta_B - \bar{\varepsilon}_T \tag{2}$$

Tailplane lift and drag referred to $\bar{\varepsilon}_T$ axes are given by

$$\left.\begin{aligned} C_{L_T}^{\bar{\varepsilon}_T} &= C_{L_T}\cos\bar{\varepsilon}_T + C_{D_T}\sin\bar{\varepsilon}_T \\ C_{D_T}^{\bar{\varepsilon}_T} &= C_{D_T}\cos\bar{\varepsilon}_T - C_{L_T}\sin\bar{\varepsilon}_T. \end{aligned}\right\} \tag{3}$$

The tailplane contribution to pitching moments has been estimated from the following expression:

$$\Delta C_{m_T} = \frac{\bar{q}_T}{q_0\,\bar{c}}\left(C_{D_T}^{B}\,h_T - C_{L_T}^{B}\,l_T\right) \tag{4}$$

where

h_T = height of tailplane mean $\frac{1}{4}$ chord point above pitch axis

l_T = distance of tailplane mean $\frac{1}{4}$ chord point behind pitch axis

$\bar{q}_T$ = mean dynamic head at tailplane

q_0 = free-stream dynamic head

$\bar{c}$ = wing mean chord used to non-dimensionalize pitching moments and $C_{D_T}^{B}$ and $C_{L_T}^{B}$ are tailplane drag and lift referred to axes parallel and normal to fuselage centreline and given by

$$\left.\begin{aligned} C_{D_T}^{B} &= C_{D_T}^{\bar{\varepsilon}_T}\cos\bar{\alpha}_T - C_{L_T}^{\bar{\varepsilon}_T}\sin\bar{\alpha}_T \\ C_{L_T}^{B} &= C_{L_T}^{\bar{\varepsilon}_T}\cos\bar{\alpha}_T + C_{D_T}^{\bar{\varepsilon}_T}\sin\bar{\alpha}_T. \end{aligned}\right\} \tag{5}$$

TABLE 1

Geometric Details of Model

Wing on Model 1	
Gross projected area	4·079 ft^2
Gross projected span	5·71 ft
Standard mean chord	0·715 ft
Aspect ratio	8
Wing-body angle	2° 36′
$\frac{1}{4}$ chord sweepback	20°
Leading-edge sweepback	22° 56′
Distance of wing root T.E. below fuselage centreline	0·219 ft
Distance of wing root T.E. behind fuselage nose	3·403 ft
Wing on Model 2	
Gross projected area	4·954 ft^2
Gross projected span	5·71 ft
Standard mean chord	0·867 ft
Aspect ratio	6·59
Wing-body angle	2° 36′
Leading-edge sweepback (centreline to 0·55 gross span)	37° 50′
Leading-edge sweepback (0·55 gross span to tip)	22° 56′
Distance of wing root T.E. below fuselage centreline	0·219 ft
Wing on Model 3	
Gross projected area	5·26 ft^2
Gross projected span	5·818 ft
Standard mean chord	0·904 ft
Aspect ratio	6·44
Wing-body angle	2° 36′
Leading-edge sweepback	37° 50′
Distance of wing root T.E. below fuselage centreline	0·219 ft
Wing on Model 4	
Details as for wing on Model 1 except that:—	
Distance of wing root T.E. above fuselage centreline	0·322 ft
Distance of wing root T.E. behind fuselage nose	3·463 ft
Wing-body angle	0°
Fuselage	
Diameter	0·72 ft
Overall length (as tested on Models 1 and 4)	5·583 ft
Overall length (as tested on Model 2)	6·333 ft
Overall length (as tested on Model 3)	7·375 ft
Tailplane 1	
Gross area	1·08 ft^2
Gross span	1·903 ft
Standard mean chord	0·568 ft
Aspect ratio	3·35
$\frac{1}{4}$ chord sweepback	25°

TABLE 1—*continued*

Distance of apex behind wing root T.E.	Position A	1·168 ft
	Position B	1·633 ft
	Position C	2·008 ft
	Position D	2·133 ft
Tailplane 2		
Gross area		1·232 ft^2
Gross span		2·284 ft
Standard mean chord		0·539 ft
Aspect ratio		4·24
$\frac{1}{4}$ chord sweepback (as tailplane 1)		25°
Height of tailplane chord above wing root T.E. (low wing position)	Position 1	1·367 ft
	Position 2	1·117 ft
	Position 3	0·867 ft
	Position 4	0·617 ft
Fin		
Height above fuselage centreline		1·25 ft
Chord (constant over span)		1·50 ft
L.E. and T.E. sweepback		26° 34′
Nacelle (small)		
Overall length		0·978 ft
Maximum diameter		0·268 ft
Internal bore (parallel)		1·6 in
Distance of nacelle intake behind wing root T.E.	Position 2	0 ft
	Position 3	0·423 ft
	Position 4	0·663 ft
Nacelle (large)		
Overall length		1·225 ft
Maximum diameter		0·43 ft
Internal bore (parallel)		3·38 in

NOTE: The appropriate values of gross wing area and standard mean chord were used to non-dimensionalize the forces and moments for each model.

TABLE 2

	Model 1 $c_R = 1{\cdot}055$ ft				Models 2 and 3 $c_R = 1{\cdot}475$ ft				
$\frac{W}{c_R}$	0·68				0·49				
$\frac{L}{c_R}$	*A*	*B*	*C*	*D*	*A*	*B*	*b*	*C*	*D*
	1·29	1·73	2·09	2·21	0·92	1·24	1·41	1·49	1·58
$\frac{H^*}{c_R}$	4	3	2	1	4	3	2	*i*	1
	0·58	0·82	1·06	1·30	0·42	0·59	0·76	0·84	0·93
$\frac{N}{c_R}$	0·93 (small), 1·16 (large)				0·66 (small), 0·83 (large)				
$\frac{l}{c_R}$	2	1, 3 and 8		4	2		3 and 5	4	6 and 7
	0	0·39		0·62	0		0·28	0·45	0·61
$\frac{n}{c_R}$	1	2, 3 and 4		8	2, 3 and 4		5	6	7
	1·19	1·21		1·47	0·86		1·10	0·91	1·09
$\frac{n}{b_T}$ T/P 1	0·66	0·67		0·81	0·67		0·85		
$\frac{n}{b_T}$ T/P 2		0·56			0·56			0·59	0·70

*For the high-wing model (4) the values of H/c_R are 0·51 less than those given for Model 1, due to the higher position of the wing on the fuselage.

TABLE 3

Aircraft	HS 121	HS 121 develop-ment	HS 125	BAC 111	VC 10	Boeing 727	DC 9	Caravelle	HS 681
W/c_R	0·49	0·49	0·62	0·68	0·38	0·46	0·65	0·52	0·63
L/c_R	1·24	1·45	1·29	1·73	1·21	1·69	2·31	1·48	1·74
H/c_R	0·84	0·84	1·03	1·06	0·85	0·90	1·22	0·59	0·86
N/c_R	0·60	0·83	0·88	0·93	0·60	0·68	1·05	0·86	—
l/c_R	0·18	0·61	−0·20	0·39	0·26	0·32	0·38	0·48	—
n/c_R	0·87	1·05	1·18	1·19	1·10	0·86	1·35	0·93	—
n/b_T	0·59	0·74	0·60	0·66	0·85	0·64	0·71	0·54	—

TABLE 4

Model	Wing	Fore body	Nacelle	Nacelle position	Tailplane	Tailplane position
1	1 (Basic configuration)	1	None	—	None	—
					1	A2, B1, B2 B3, B4, D1 D2
			1	1	None	—
					1	B2
				2	None	—
					1	B2, B3, D1 D2
				3	None	—
					1	A2, B2
				4	None	—
					1	B2
				8	None	—
					1	B2
		2	None	—	None	—
					1	B2
2	2	2	None	—	None	—
					1	B1, B2, B3 B4, C3, D1
			1	2	None	—
					1	B1, B2, D1
				3	None	—
					1	B2, D1
				4	None	—
					1	B2, C3, D1
				5	None	—
					1	B2
4	1 (High wing arrangement)	1	None	—	None	—
					1	B1, B2, B3 B4, D1, D2
1	1 (Basic configuration)	1	None	—	2	B1, B2, B3 B4, D1, D2
			1	1	2	B2
				2	2	B2, D1, D2
				3	2	B2
				4	2	B2
2	2	2	1	2	2	D1

TABLE 4—*continued*

Model	Wing	Fore body	Nacelle	Nacelle position	Tailplane	Tailplane position
3	3	3	None	—	None	—
					2	bi
			2	6	2	bi
				7	2	bi
1	1 (Wing flaps 0°)	1	1	1	1	B2

For most of the tailplane positions listed at least two settings of the tailplane, $\eta_B = 0$ and $-10°$, were used.

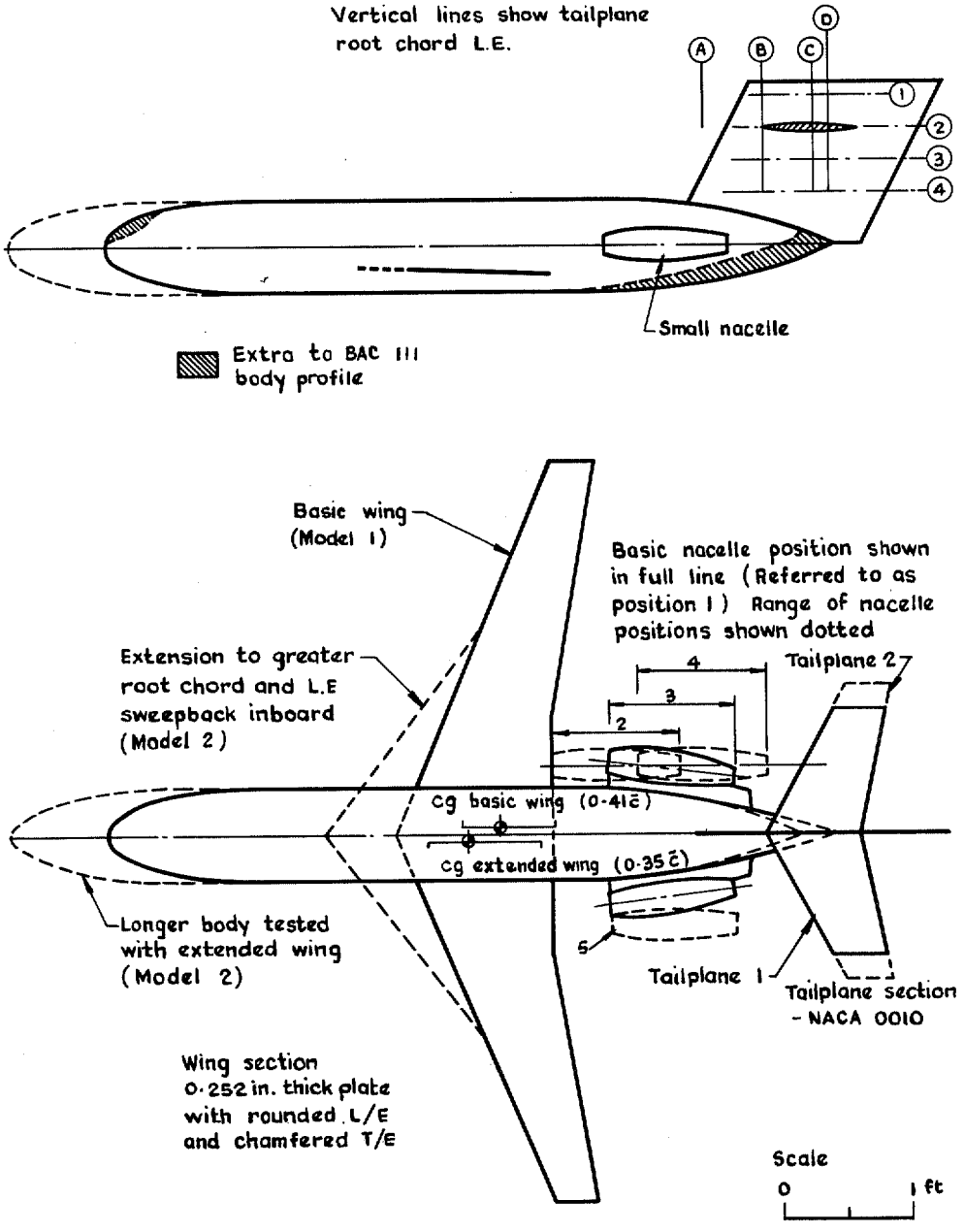

FIG. 1. GA of Models 1 and 2.

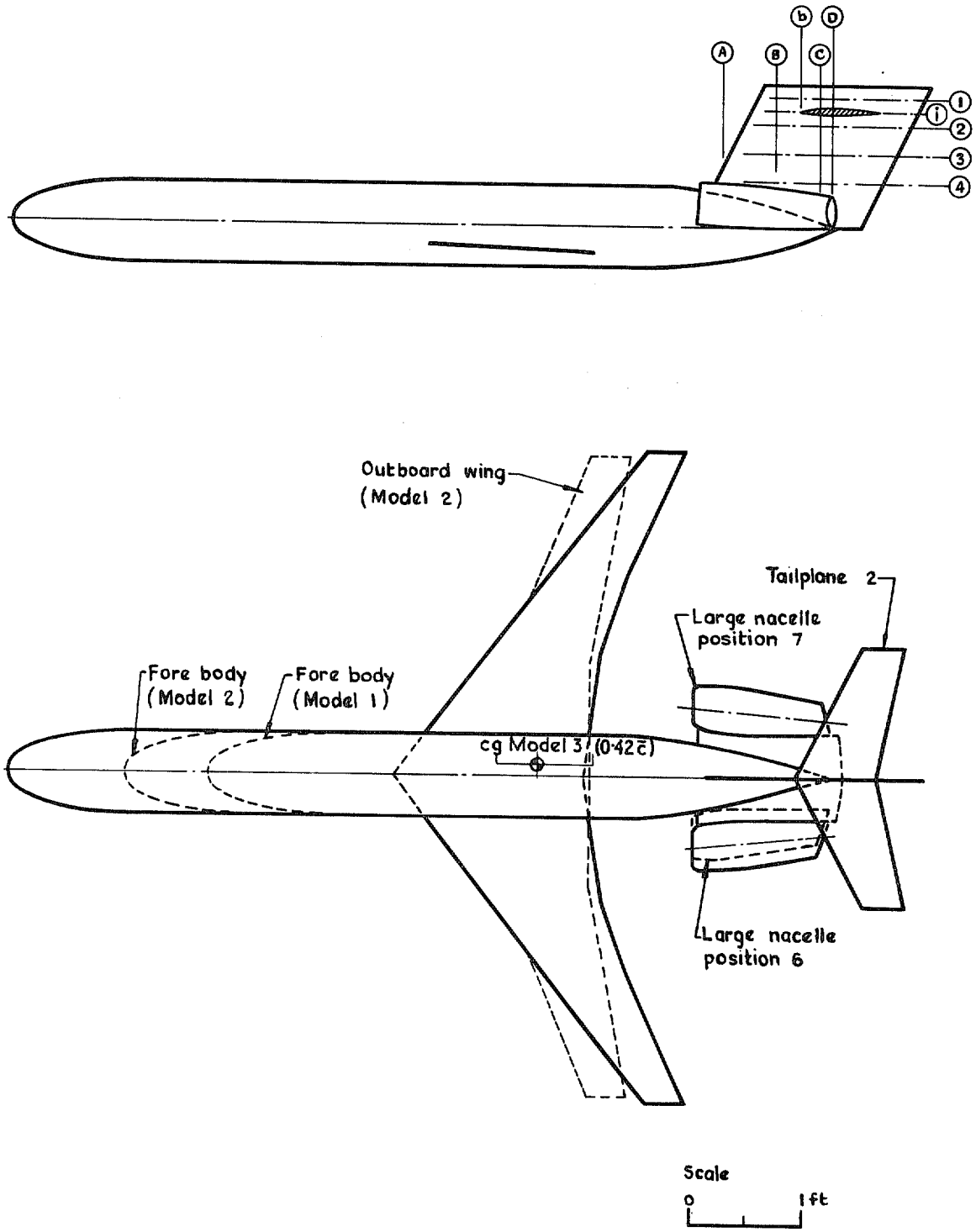

FIG. 2. GA of Model 3.

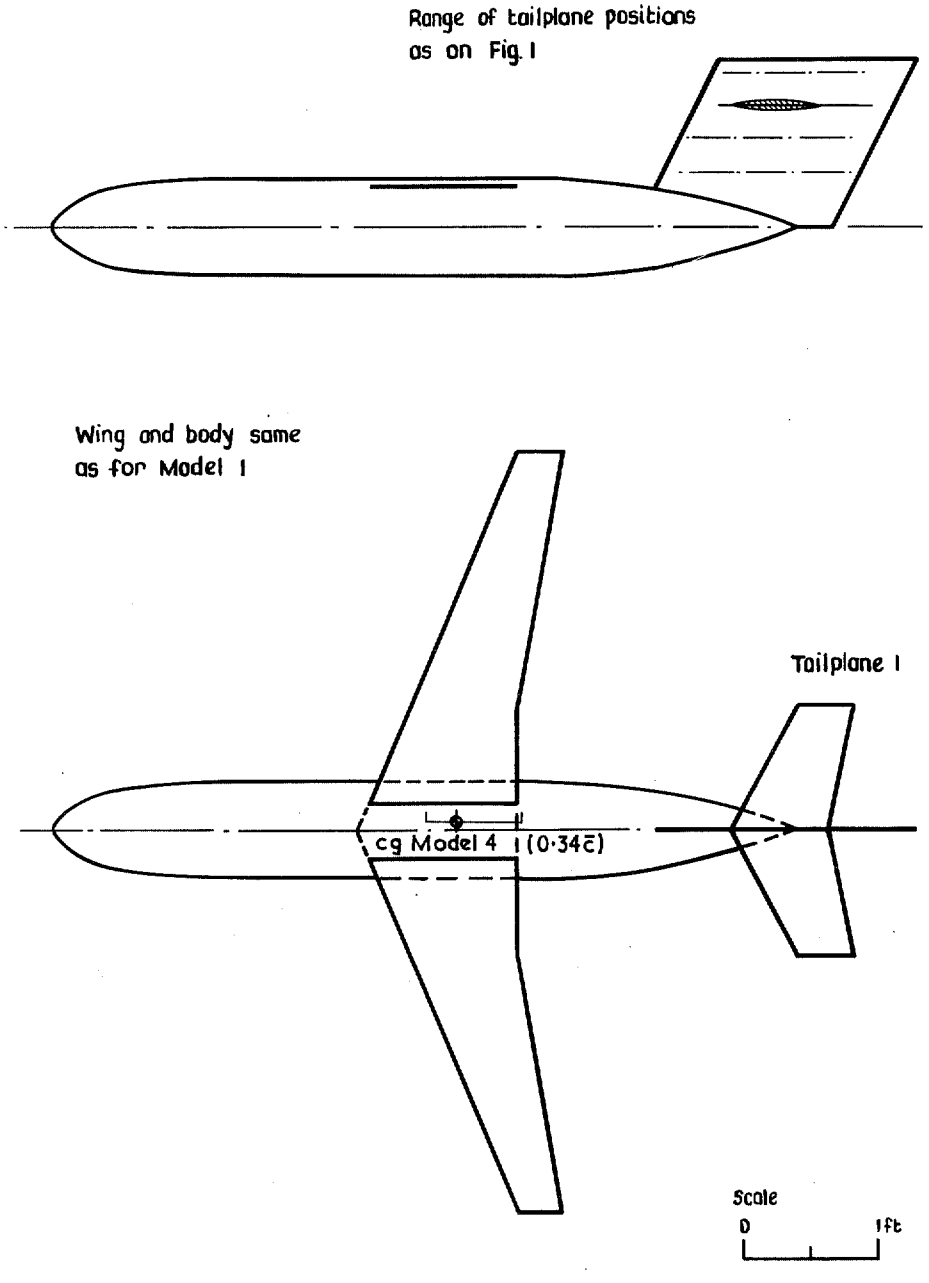

FIG. 3. GA of highwing configuration – Model 4.

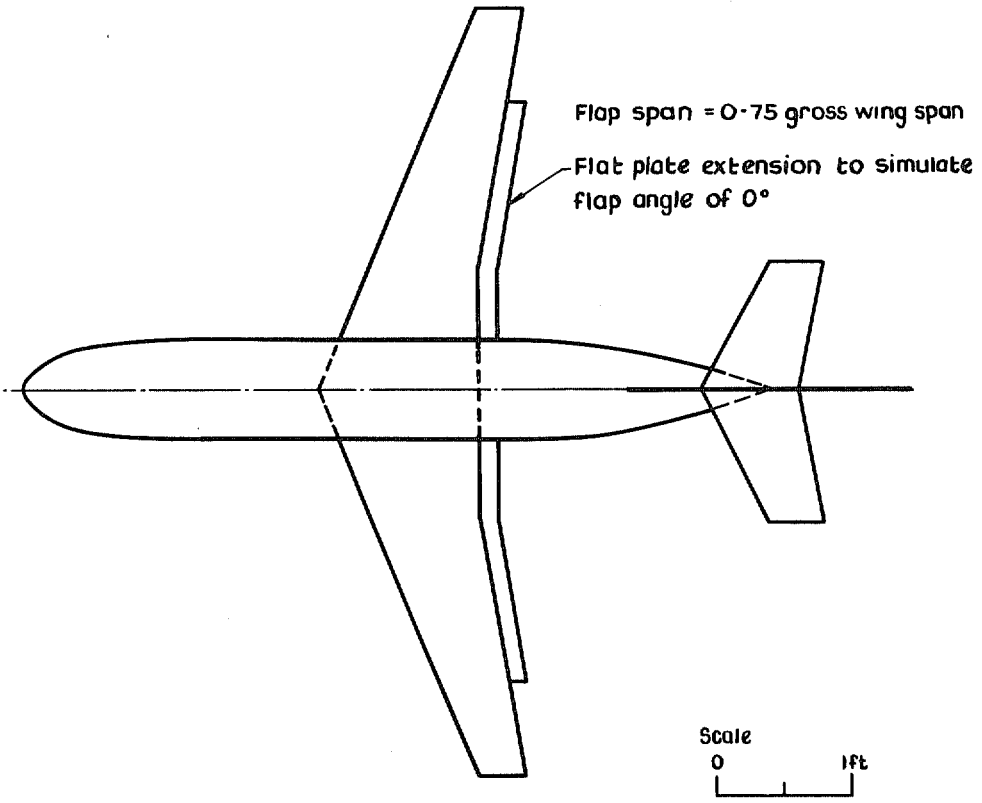

FIG. 4. Flap geometry tested on Model 1.

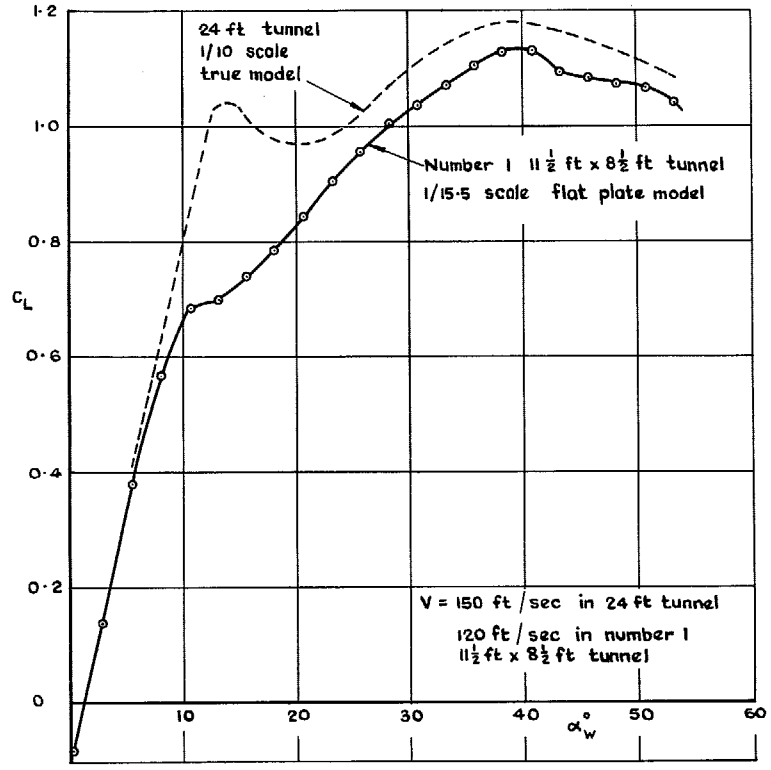

FIG. 5 a & b. Comparison between flat plate and true Models of BAC 111. $\eta_B = 0°$, nacelles on.

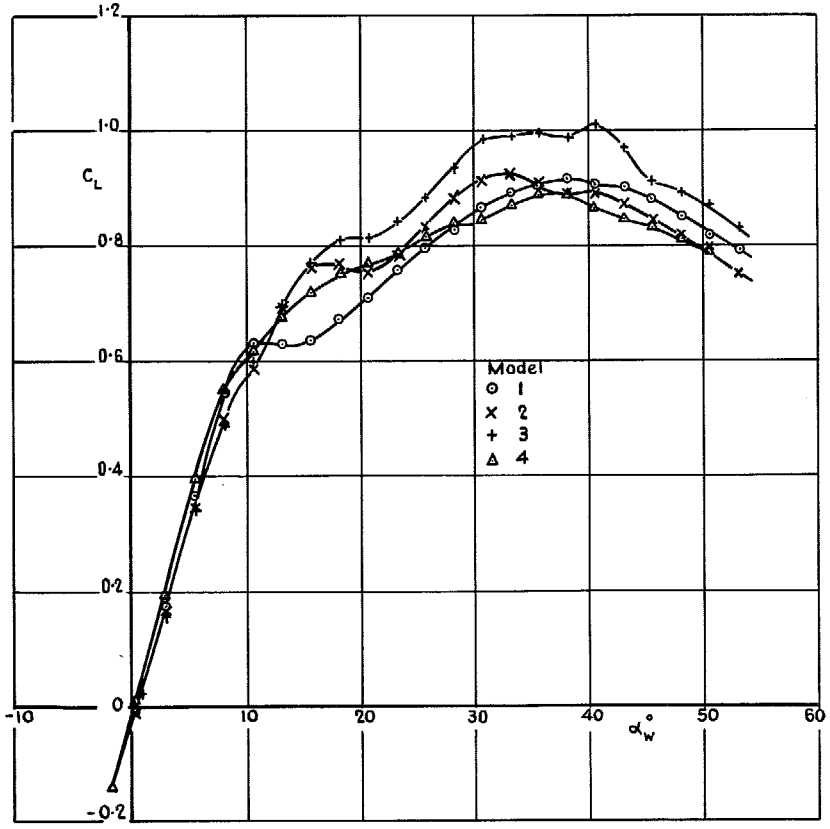

FIG. 6. Lift coefficient for various models. No nacelles; no tailplane.

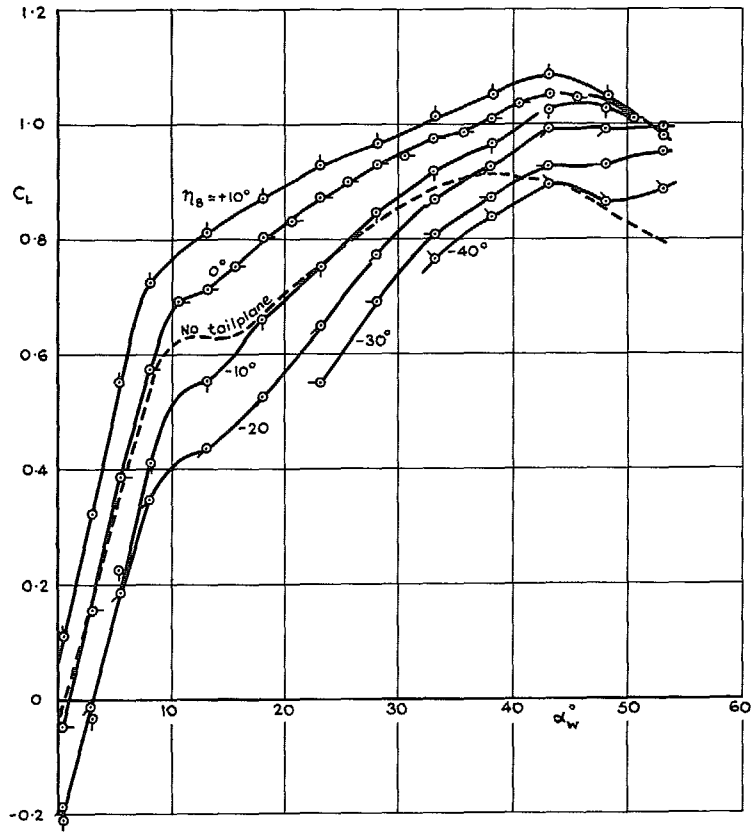

FIG. 7. C_L vs. α_w; Tailplane setting η_B varied.
No nacelles; Tailplane 1, position B2, Model 1.

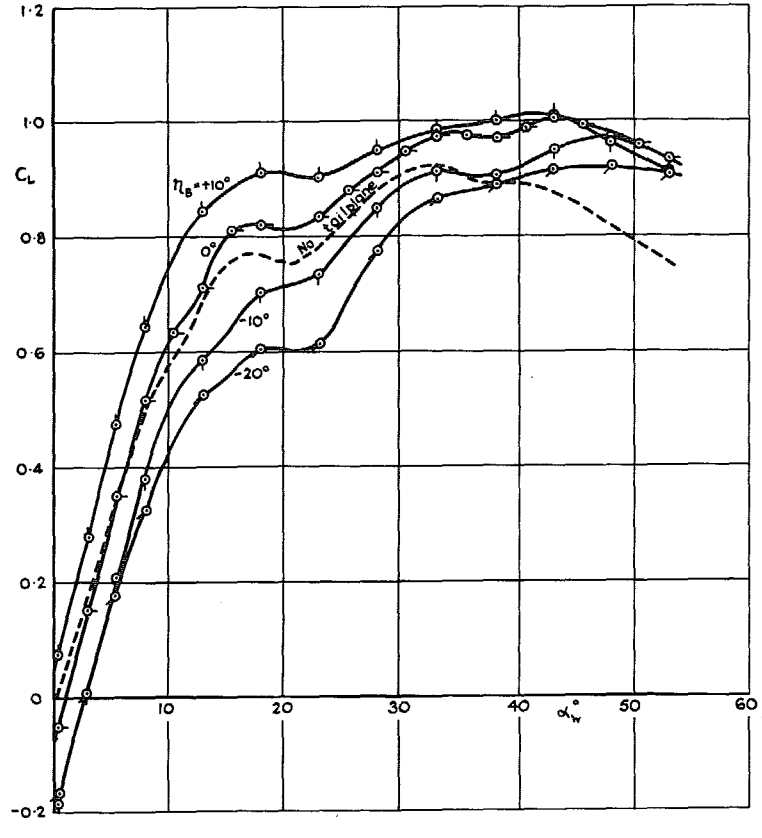

FIG. 8. C_L vs. α_w; Tailplane setting η_B varied.
No nacelles; Tailplane 1, position B2, Model 2.

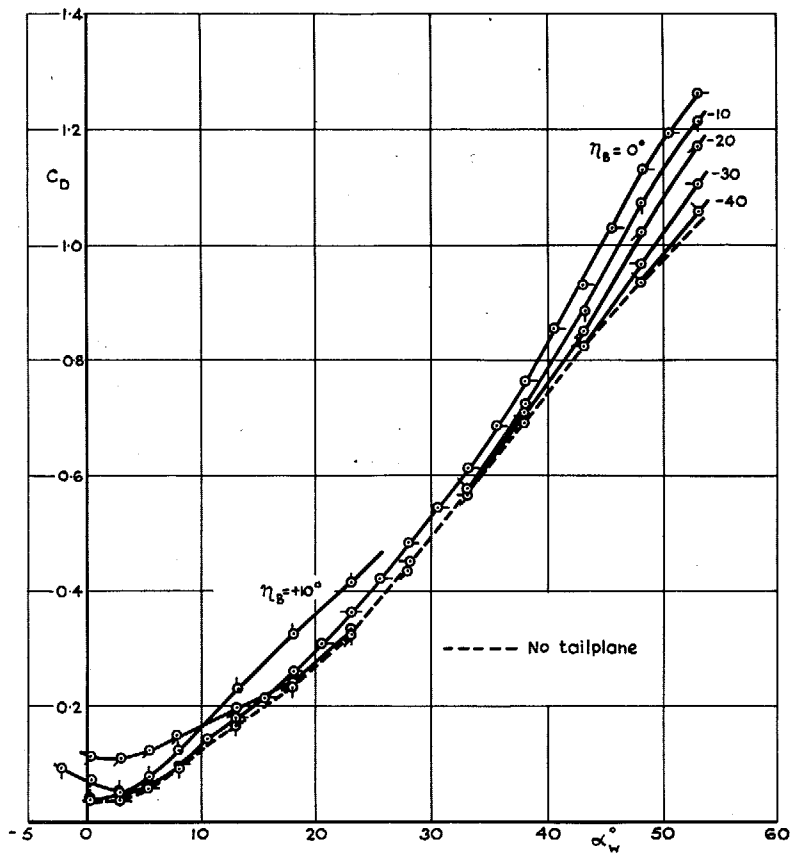

FIG. 9. C_D vs. α_w; Tailplane setting η_B varied. No nacelles; Tailplane 1, position B2, Model 1.

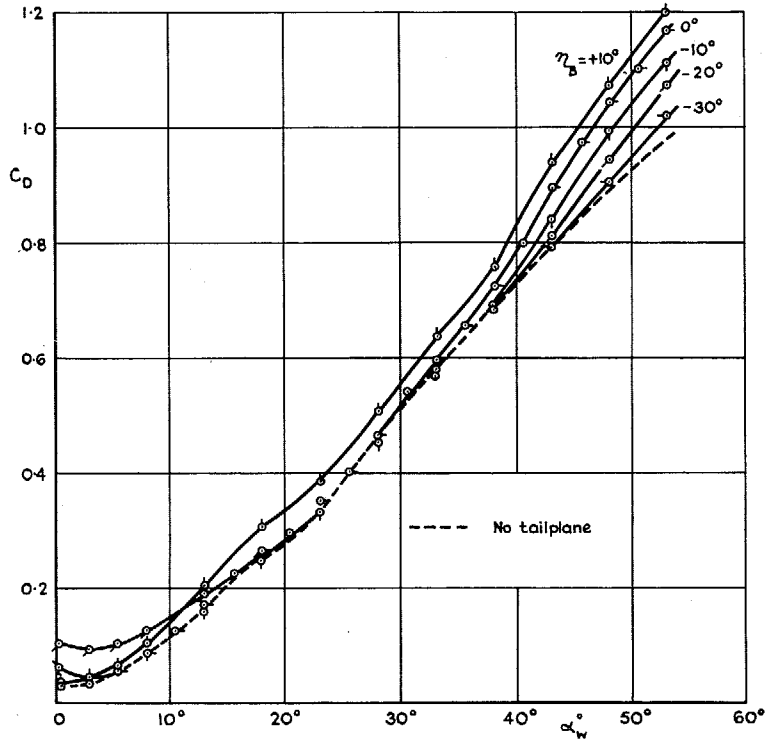

FIG. 10. C_D vs. α_w; Tailplane setting η_B varied. No nacelles; Tailplane 1, position B2, Model 2.

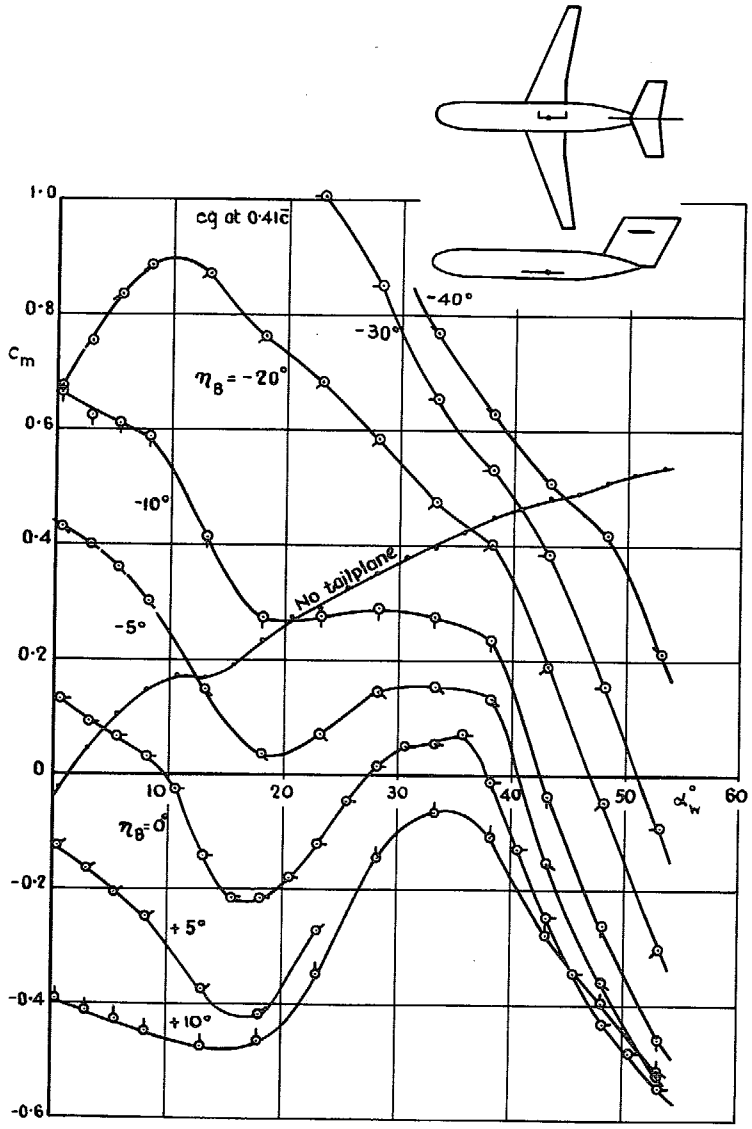

FIG. 11. C_m vs. α_w; Tailplane setting η_B varied.
No nacelles; Tailplane 1, position B2, Model 1.

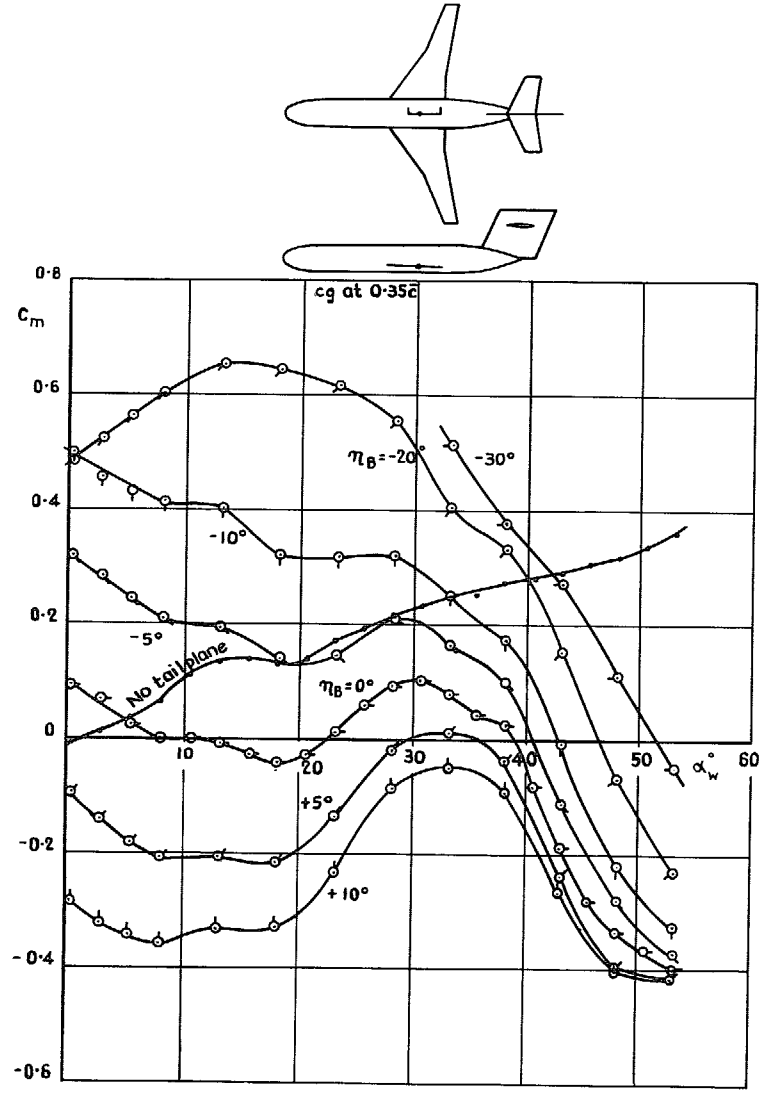

FIG. 12. C_m vs. α_w; Tailplane setting η_B varied.
No nacelles; Tailplane 1, position B2, Model 2.

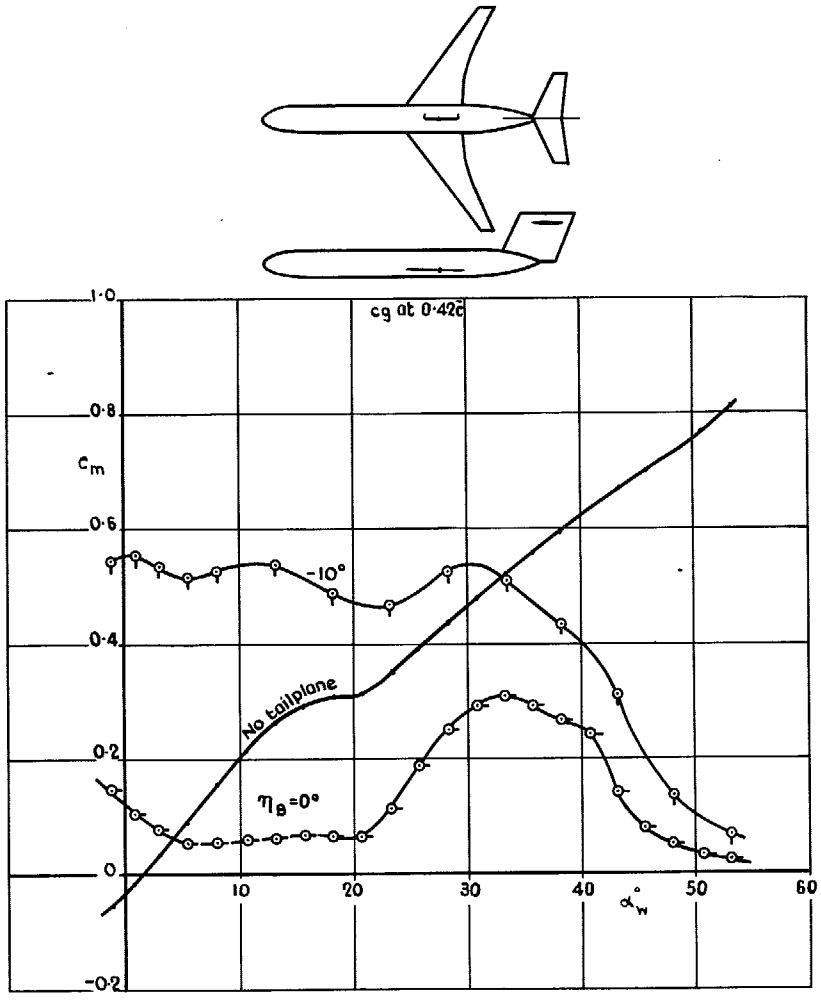

FIG. 13. C_m vs. α_w; Tailplane setting η_B varied.
No nacelles; Tailplane 2, position *bi*, Model 3.

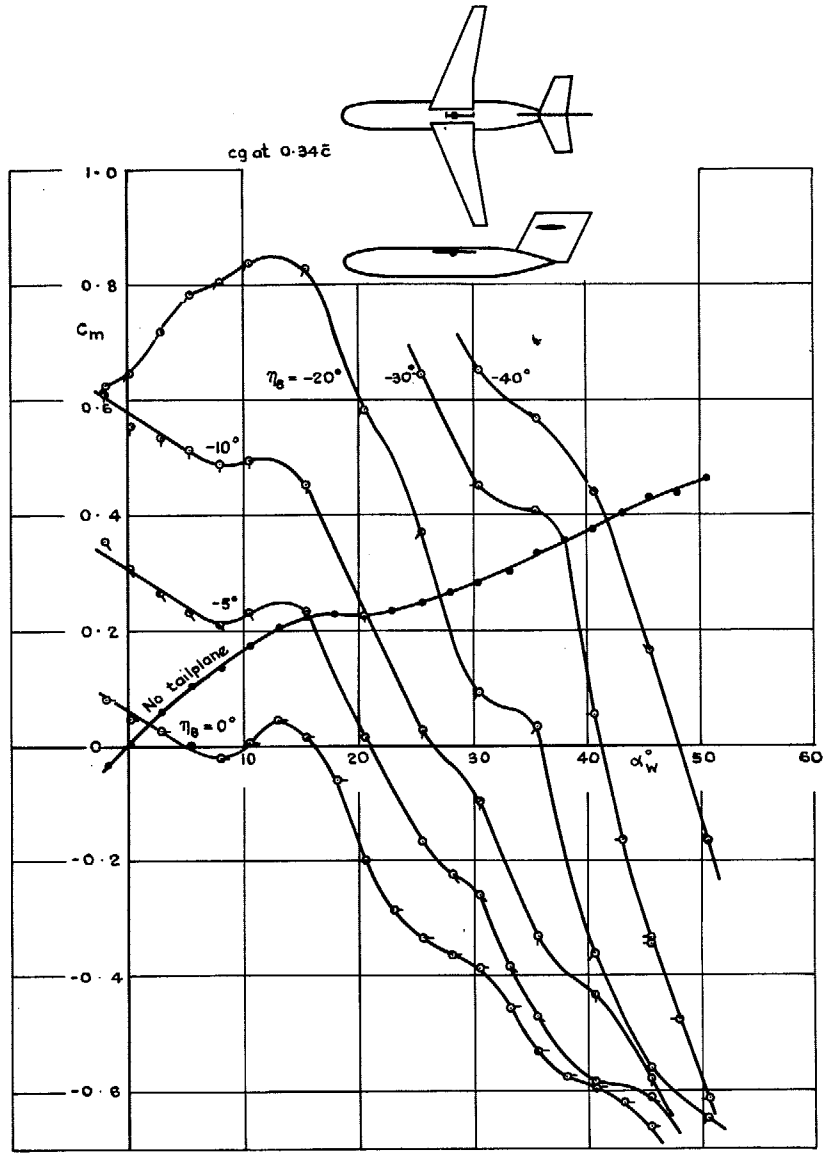

FIG. 14. C_m vs. α_w; Tailplane setting η_B varied.
No nacelles; Tailplane 1, position B2, Model 4.

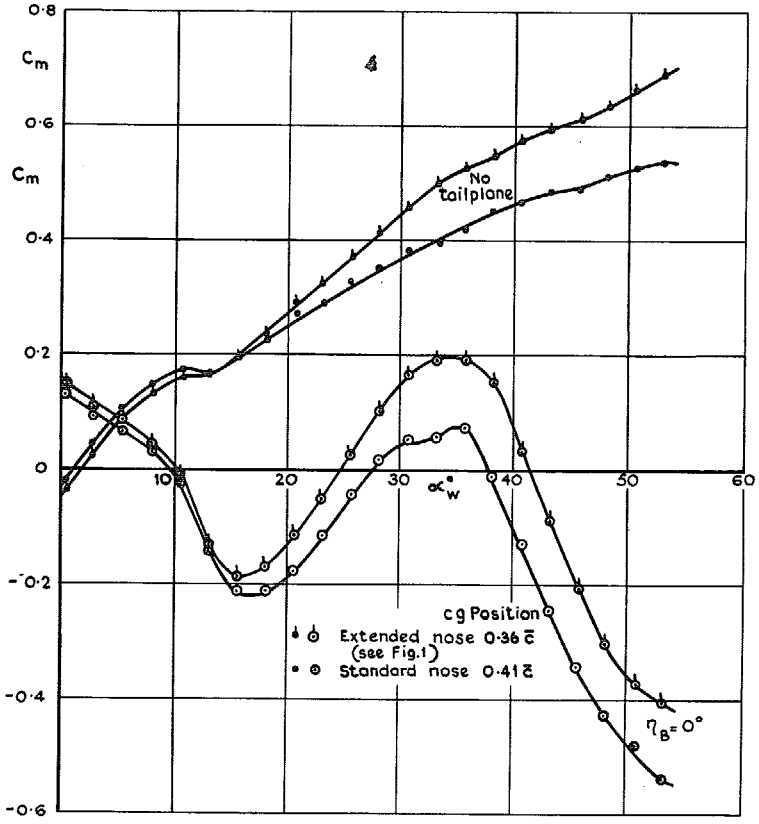

FIG. 15. Effect of fuselage forward extension on C_m. No nacelles; Tailplane 1, position B2, Model 1, Wing 1.

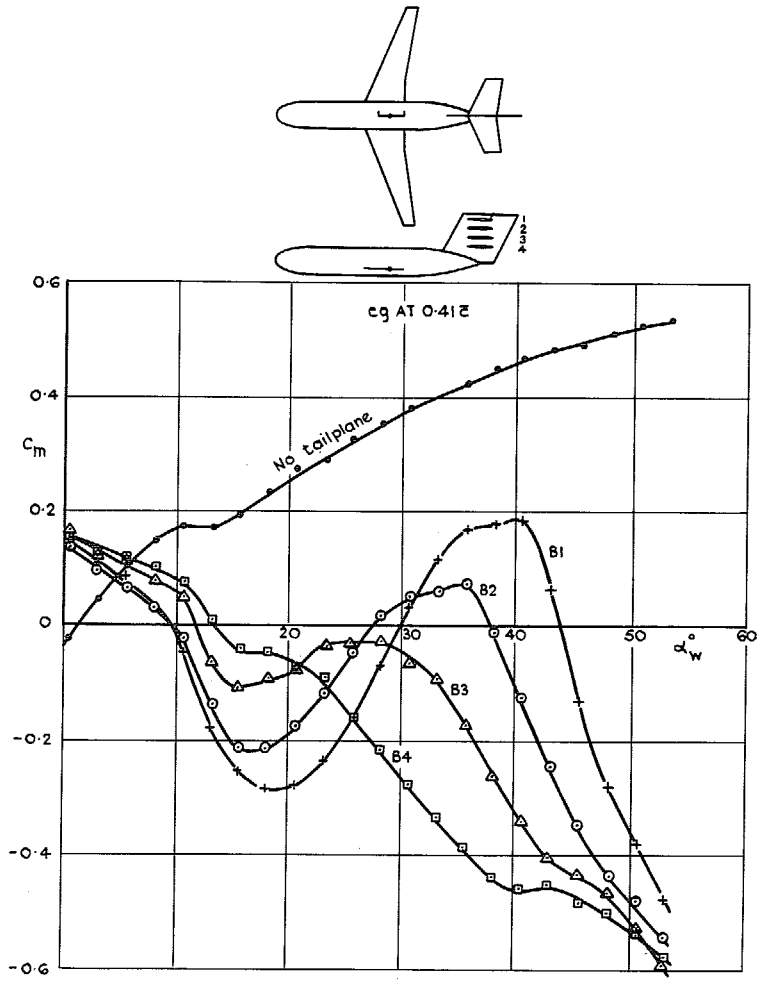

FIG. 16. Effect of vertical location of Tailplane 1 on C_m. No nacelles; Model 1.

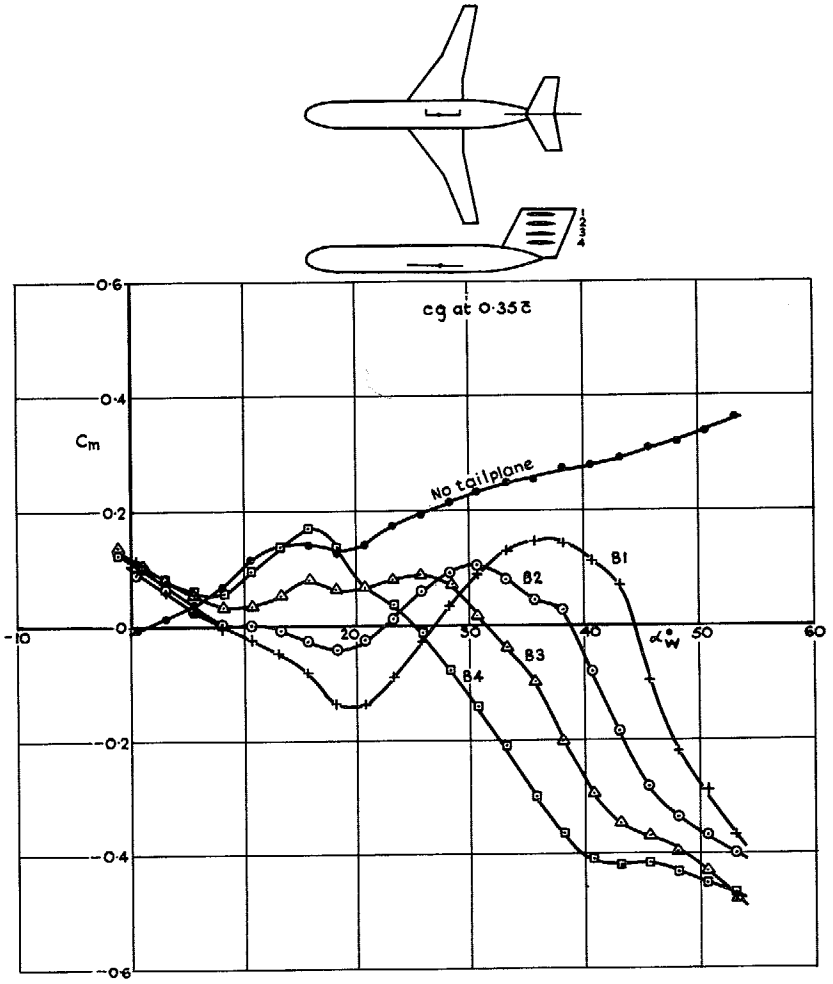

FIG. 17. Effect of vertical location of Tailplane 1 on C_m.
No nacelles; Model 2.

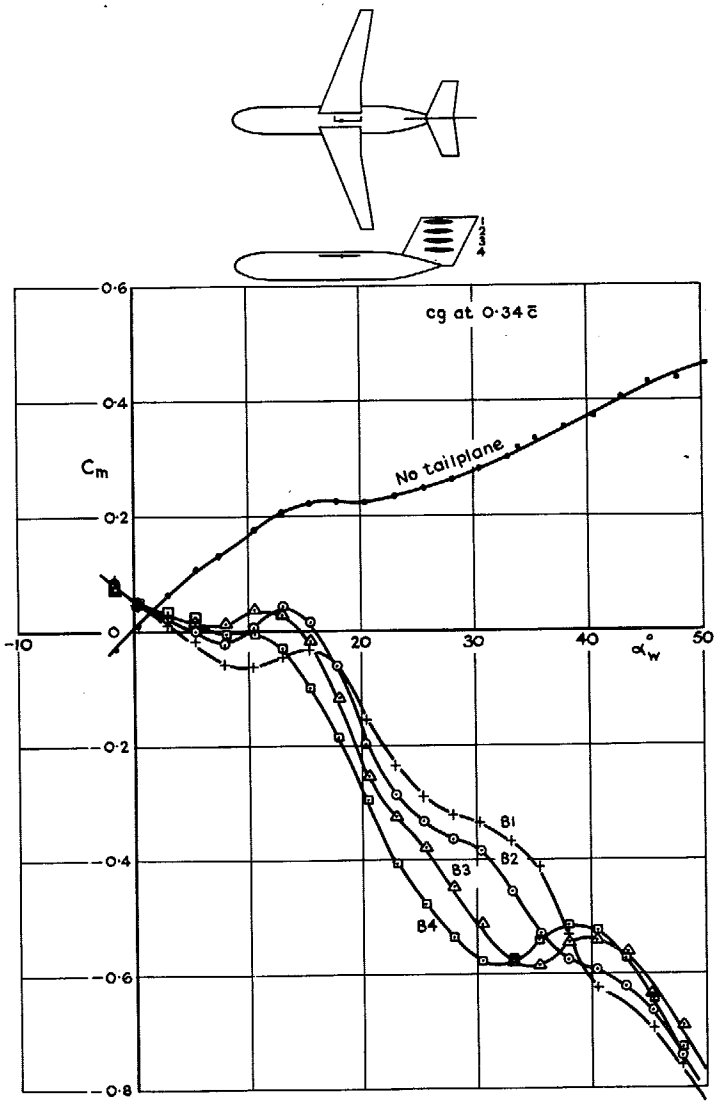

FIG. 18. Effect of vertical location of Tailplane 1 on C_m.
No nacelles; Model 4.

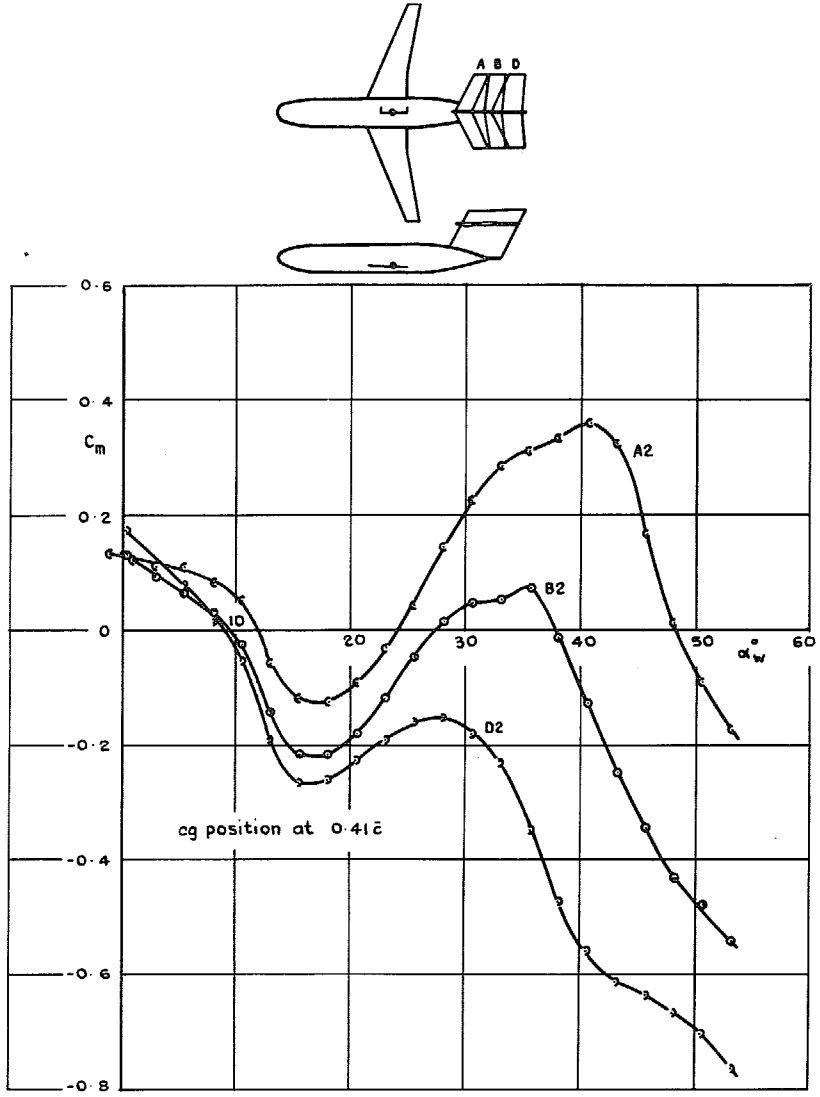

FIG. 19. Effect of tail arm on C_m (Tailplane 1). No nacelles; Model 1, constant cg position.

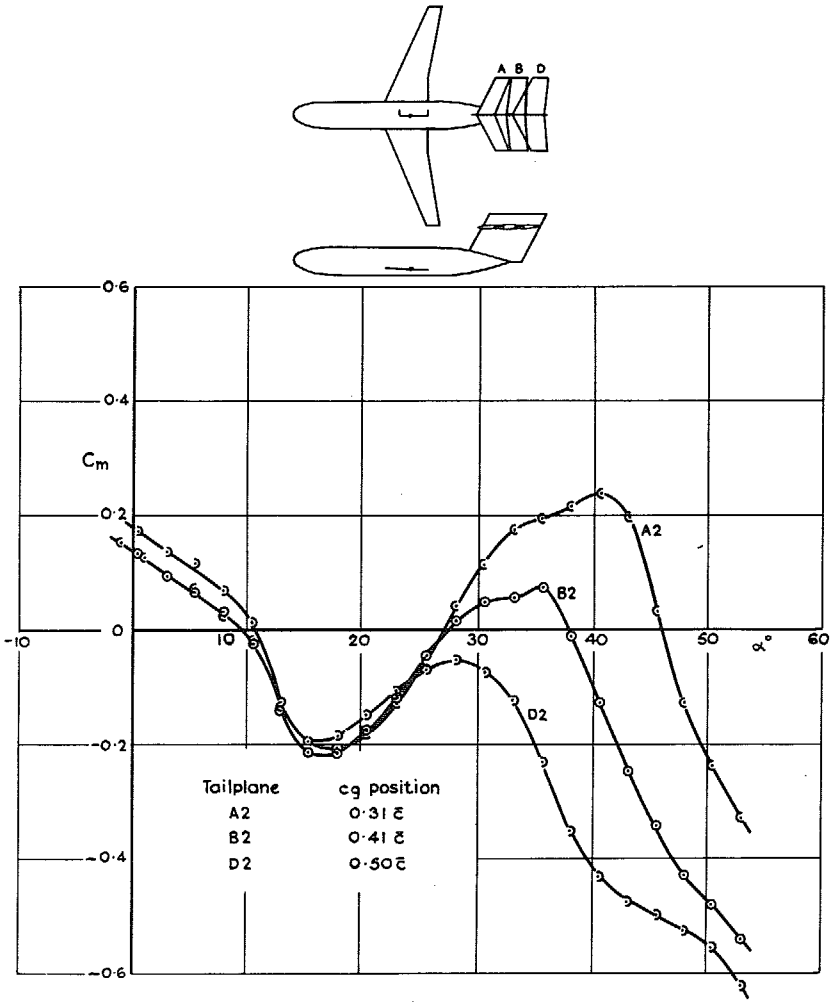

FIG. 20. Effect of tail arm on C_m (Tailplane 1). No nacelles; Model 1, cg positions adjusted for constant stability margin at low incidence.

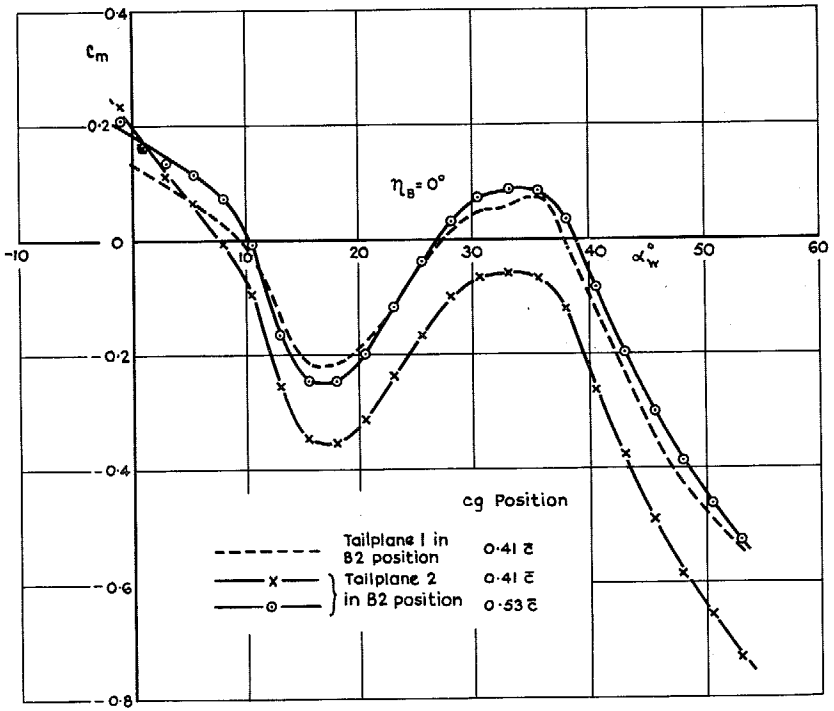

FIG. 21. Effect of 20 per cent larger tailplane span on C_m with and without cg adjustment.

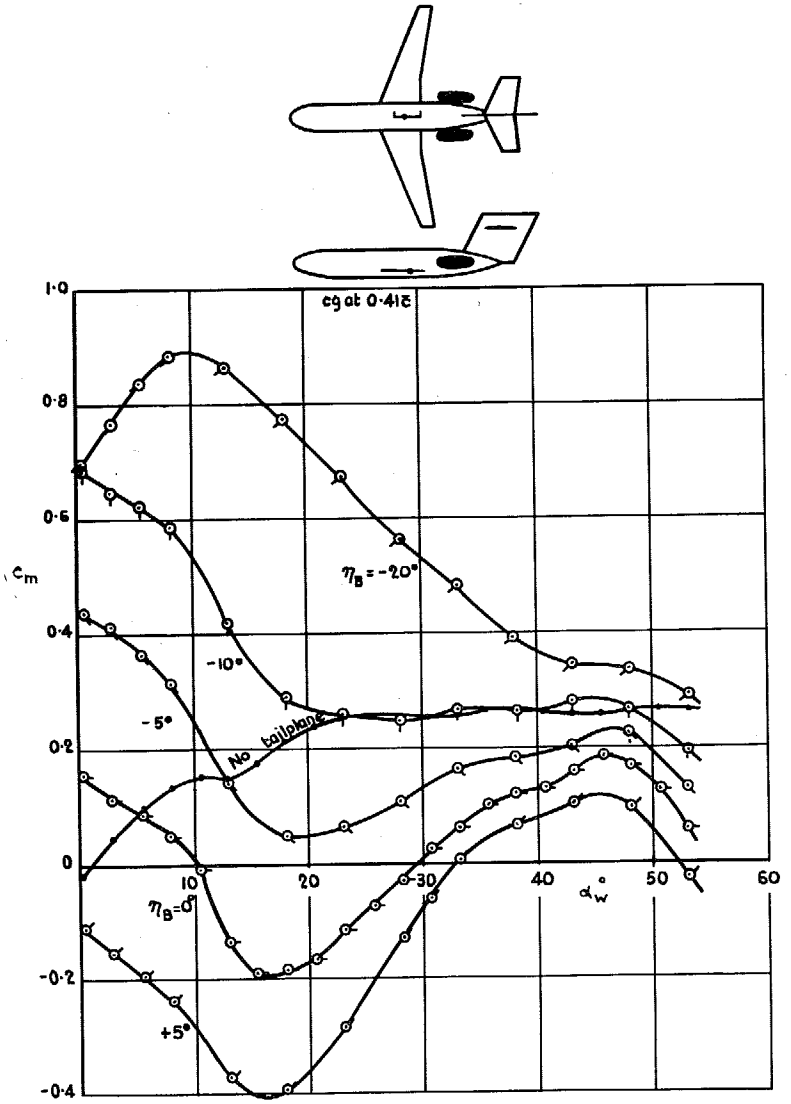

FIG. 22. C_m vs. α_w. Tailplane setting η_B varied. Small nacelles, position 1; Tailplane 1, position B2; Model 1.

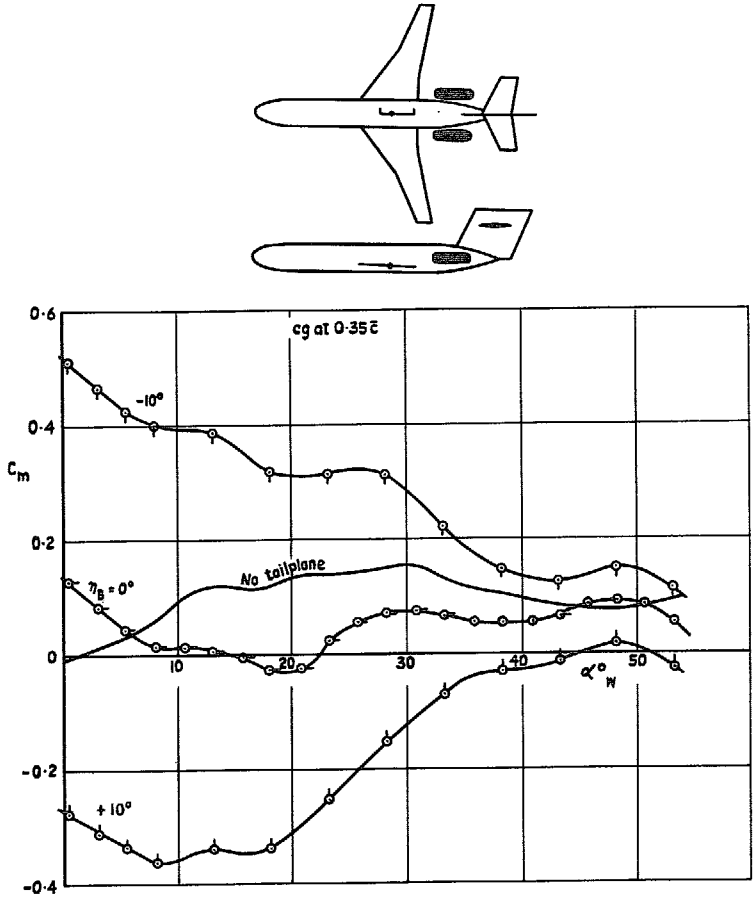

FIG. 23. C_m vs. α_w. Tailplane setting η_B varied. Small nacelles, position 3; Tailplane 1, position B2; Model 2.

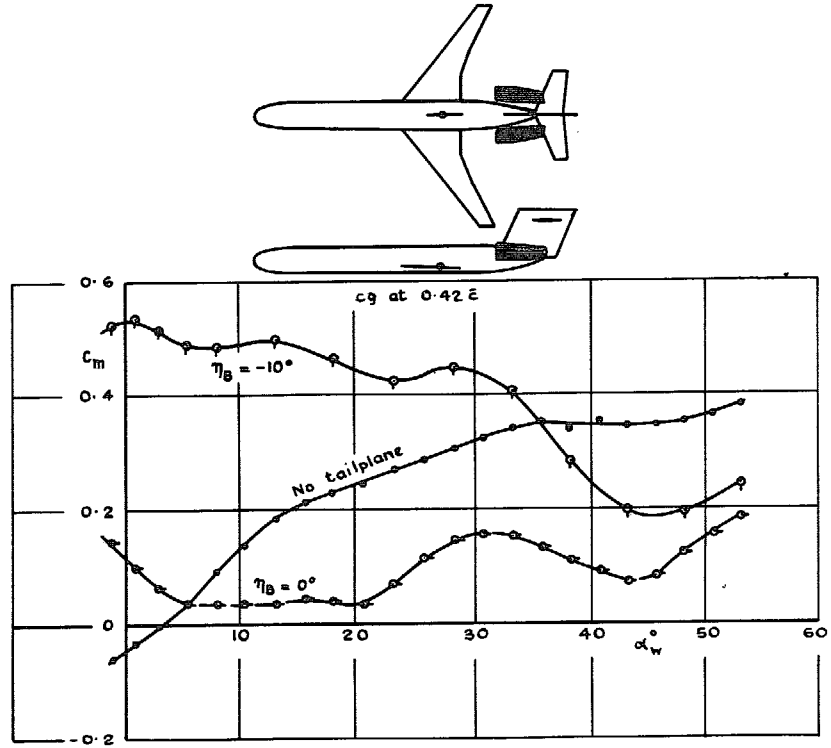

FIG. 24. C_m vs. α_w; Tailplane setting η_B varied; Large nacelles, position 7; Tailplane 2, position bi. Model 3.

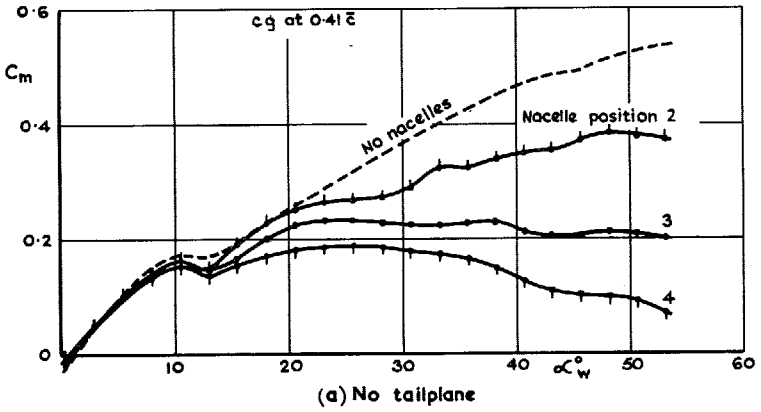

(a) No tailplane

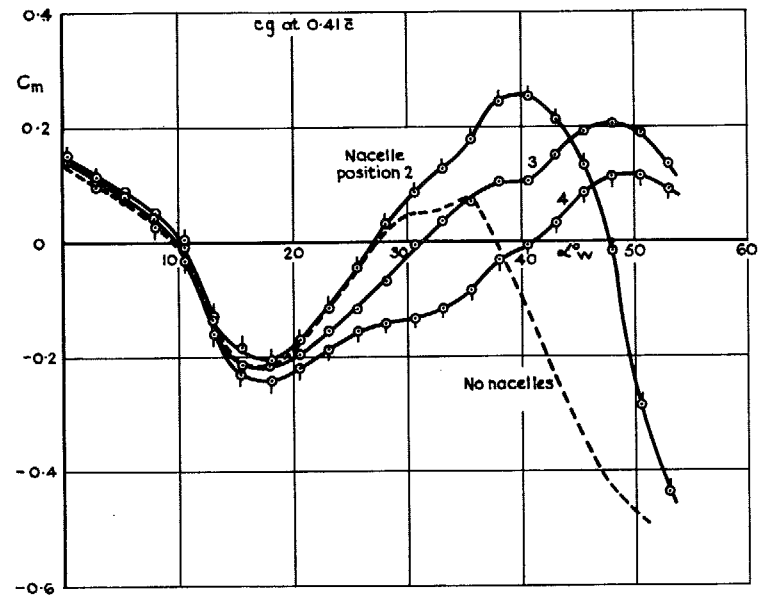

(b) With tailplane 1, Position B2

FIG. 25a & b. Effect of fore and aft location of small nacelles on C_m; Model 1.

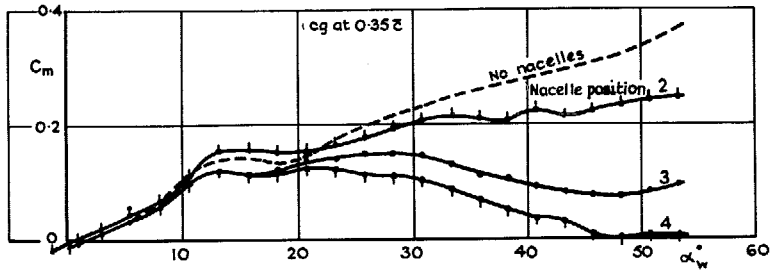

(a) No tailplane

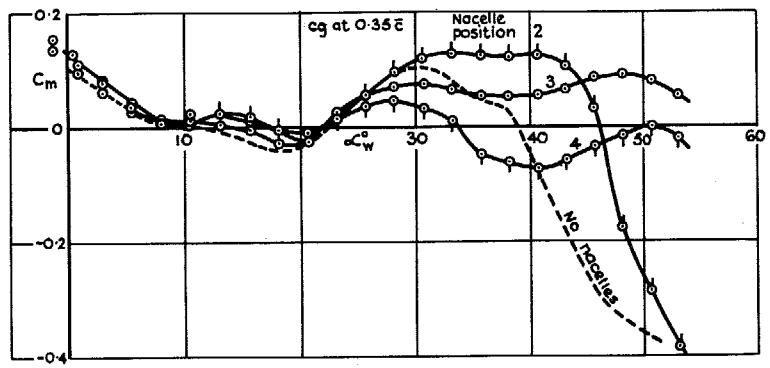

(b) With tailplane 1, Position B2

FIG. 26a & b. Effect of fore and aft location of small nacelles on C_m; Model 2.

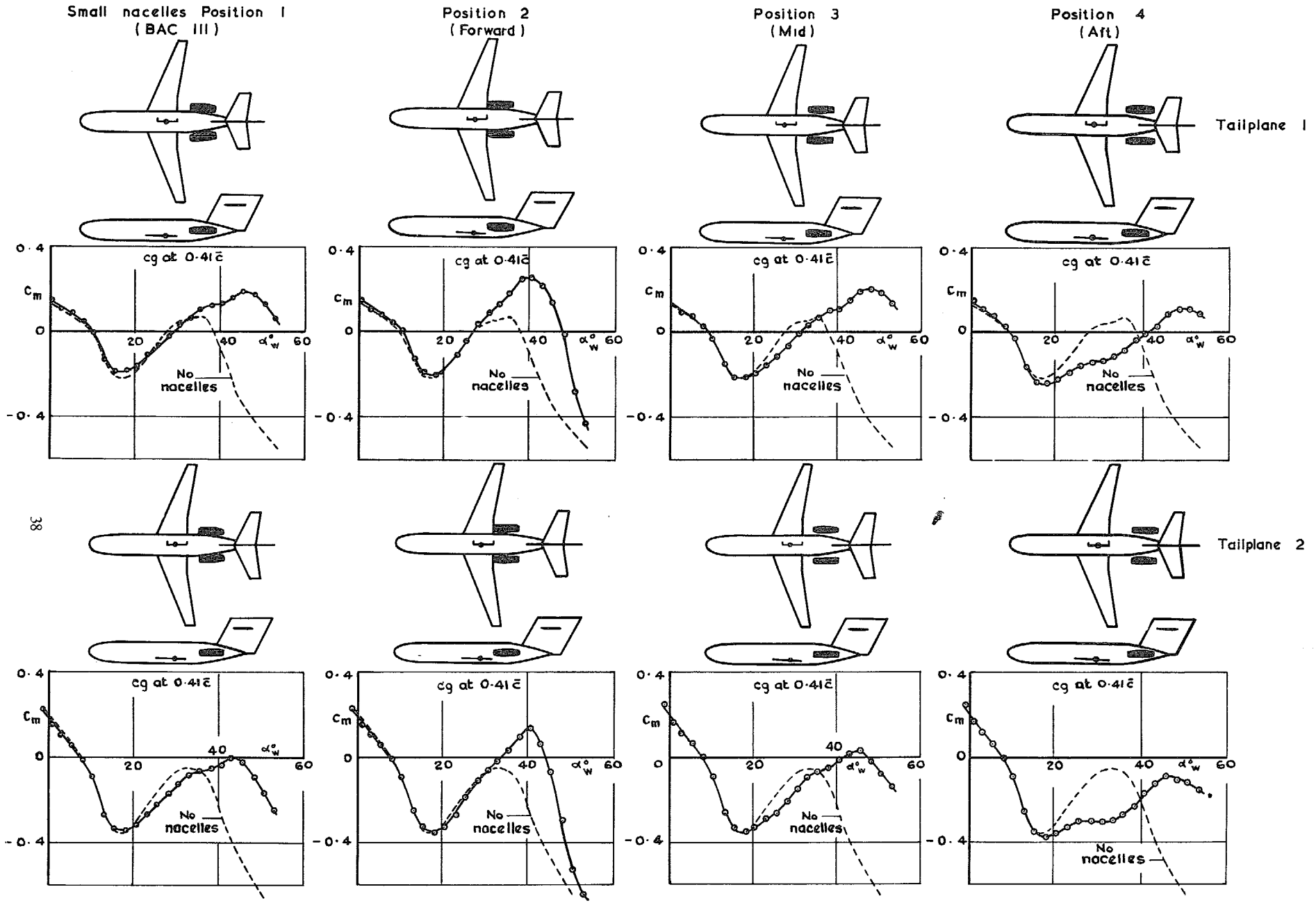

FIG. 27. Effect of fore and aft location of nacelles. Tailplanes 1 and 2 (B2 position); Model 1.

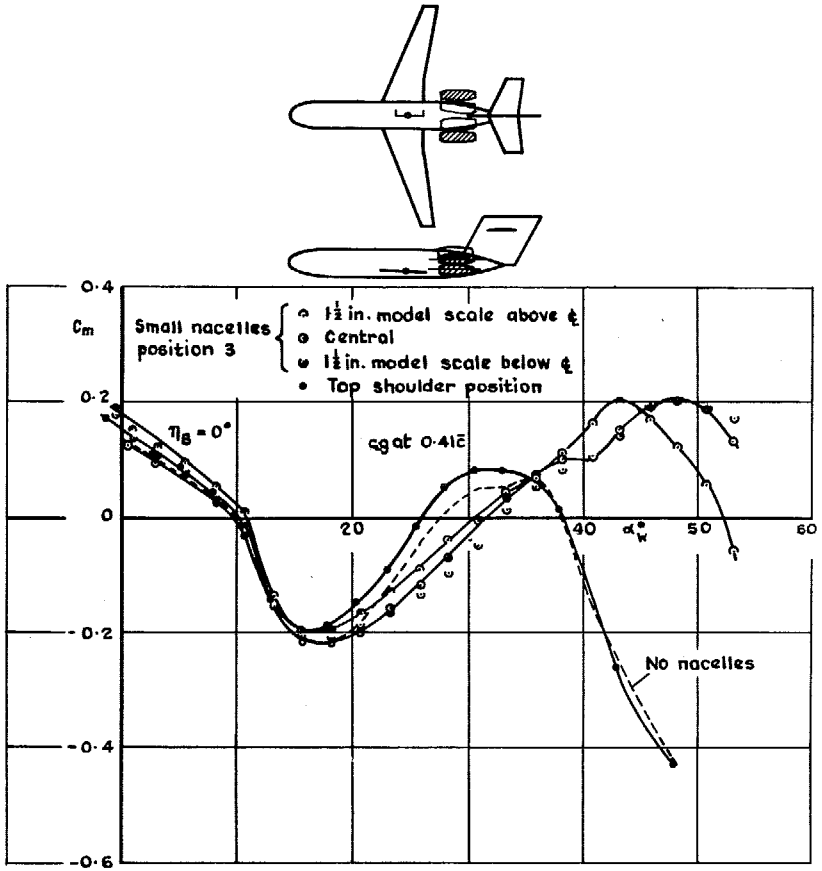

FIG. 28. Effect of vertical location of nacelles. Tailplane 1, position B2; Model 1.

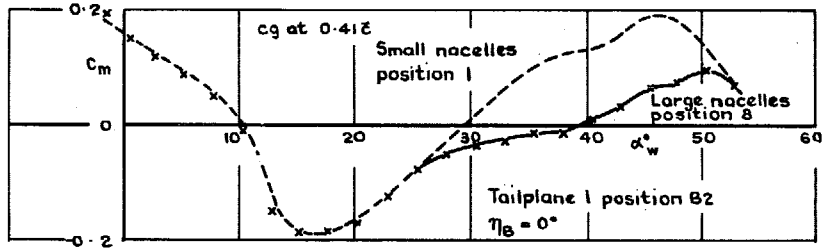

(a) Comparison of nacelle size; Model 1.

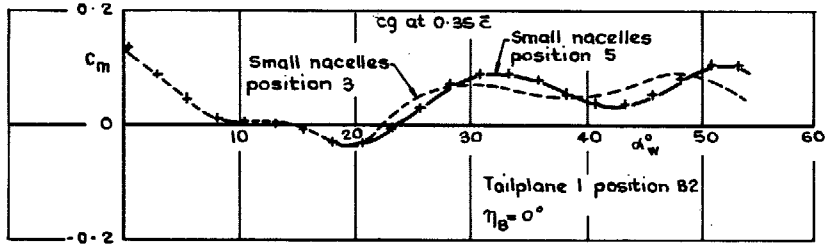

(b) Comparison of nacelle span; Model 2.

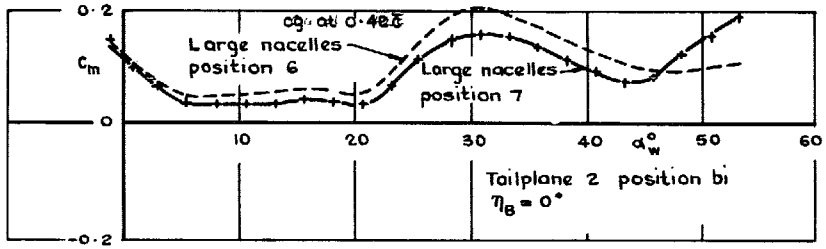

(c) Comparison of nacelle span; Model 3.

FIG. 29a to c.

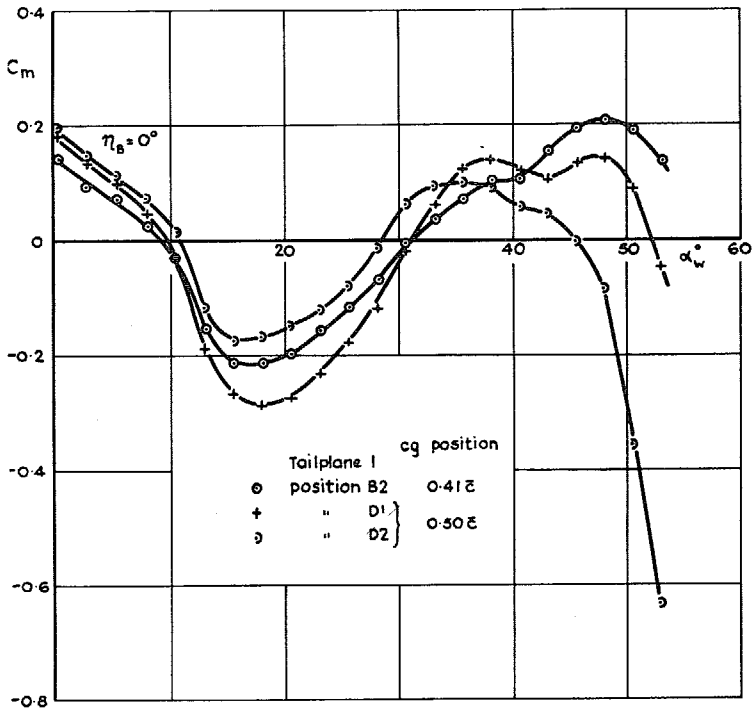

FIG. 30. Comparison of alternative tail positions. Small nacelles position 3; Model 1; cg positions adjusted for constant stability margin at low incidence.

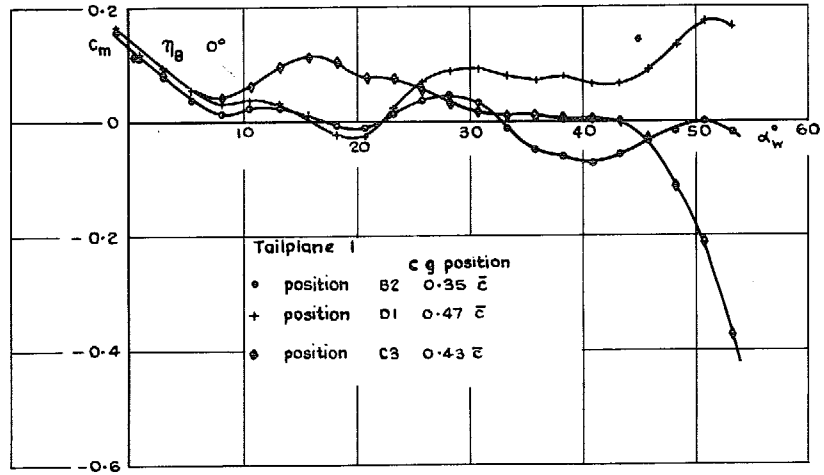

FIG. 31. Comparison of alternative tail positions. Small nacelles position 4; Model 2; cg positions adjusted for constant stability margin at low incidence.

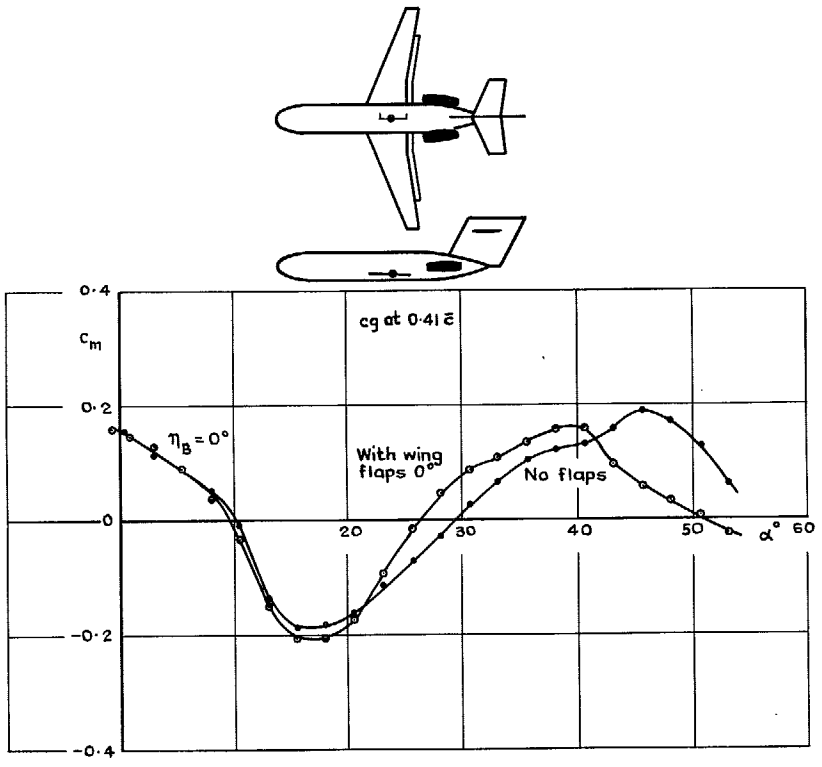

FIG. 32. Effect of wing flap extension (0° deflection). Small nacelles position 1; Tailplane 1, position B2; Model 1.

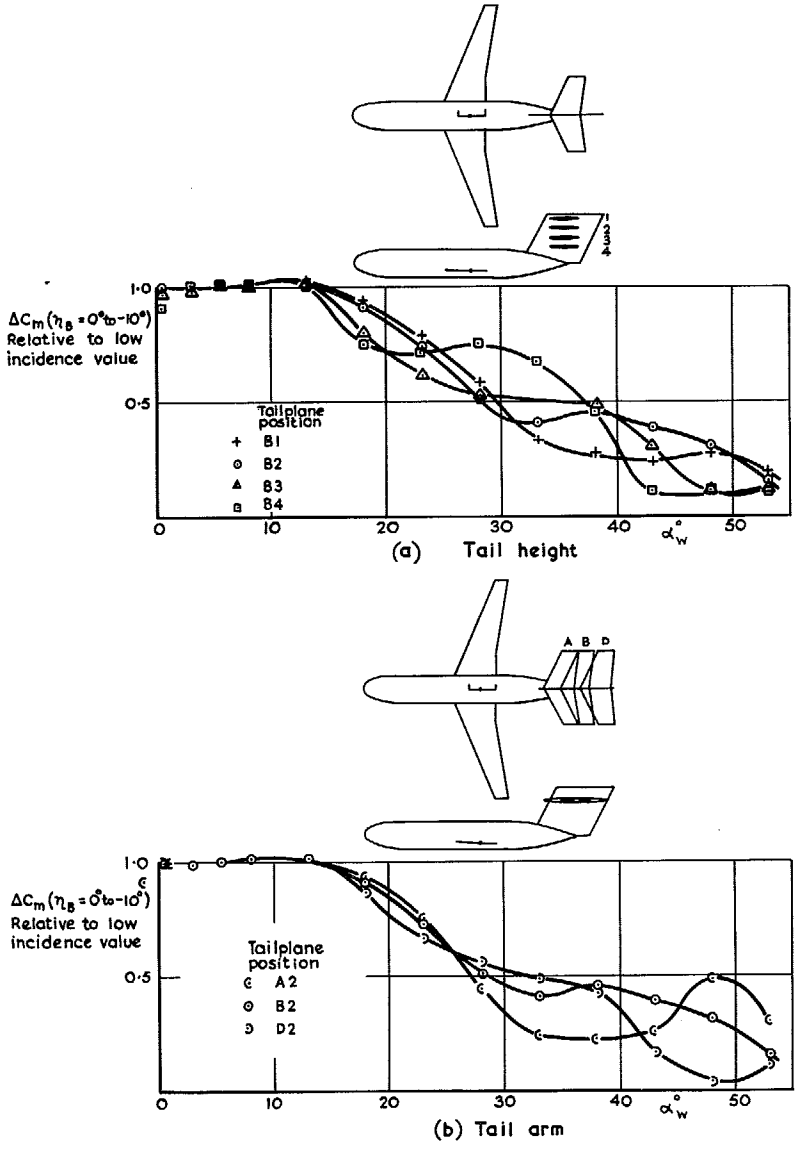

FIG. 33a and b. Relative tailplane effectiveness for vertical and fore and aft positions of tailplane 1. No nacelles; Model 1.

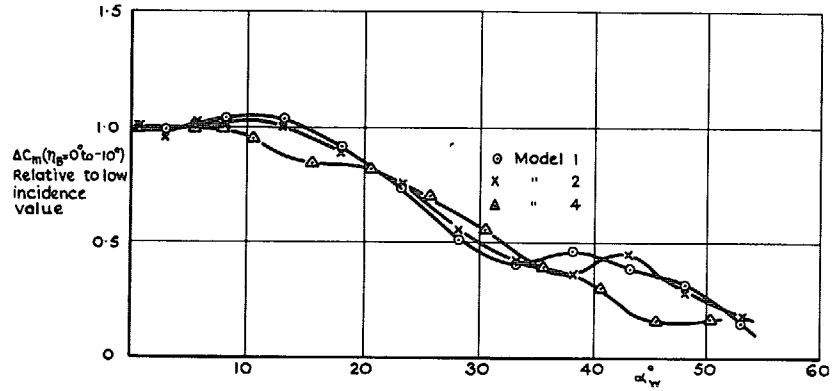

FIG. 34. Relative tailplane effectiveness with Models 1, 2 and 4. No nacelles; Tailplane 1, position B2.

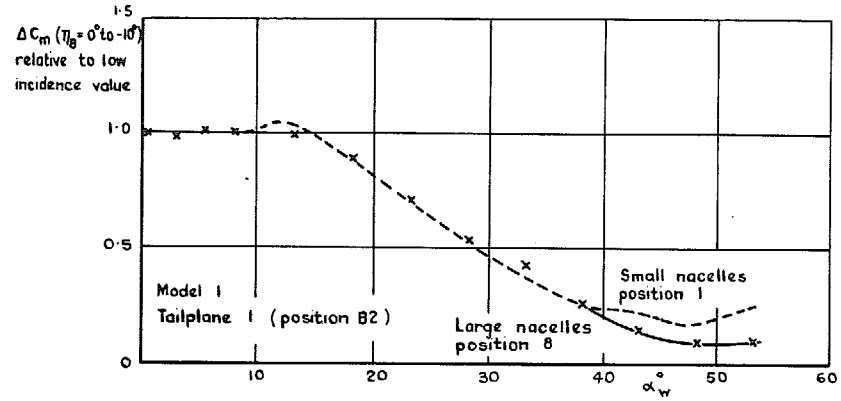

(b) Nacelle size

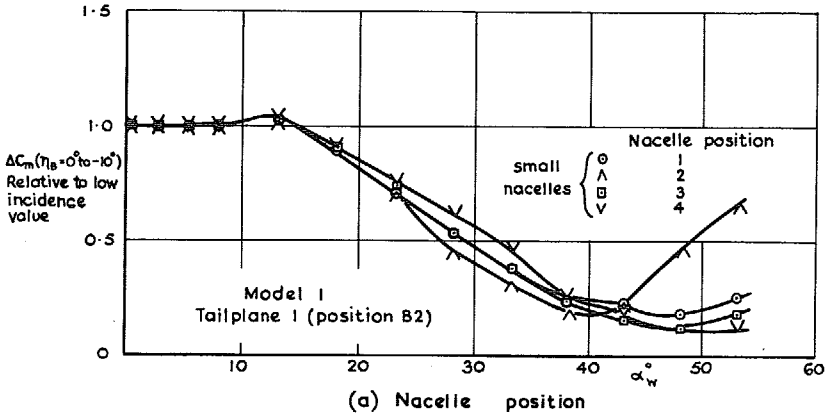

(a) Nacelle position

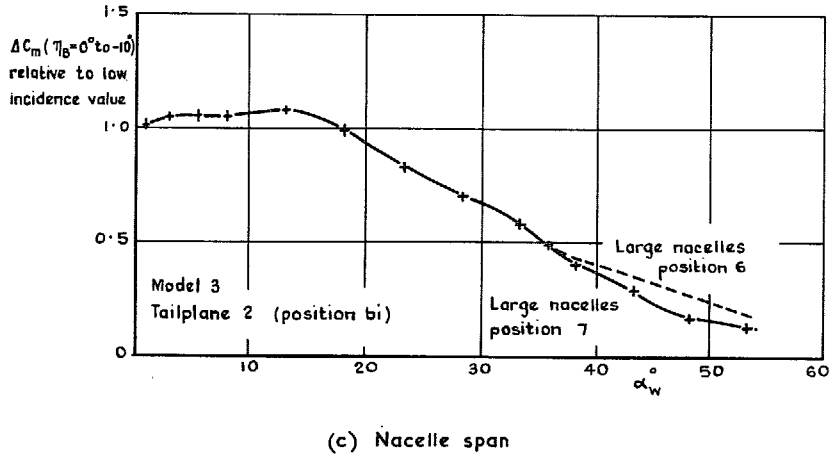

(c) Nacelle span

FIG. 35a. Effect of nacelles on tailplane effectiveness.

FIG. 35b and c. Effect of nacelles on tailplane effectiveness.

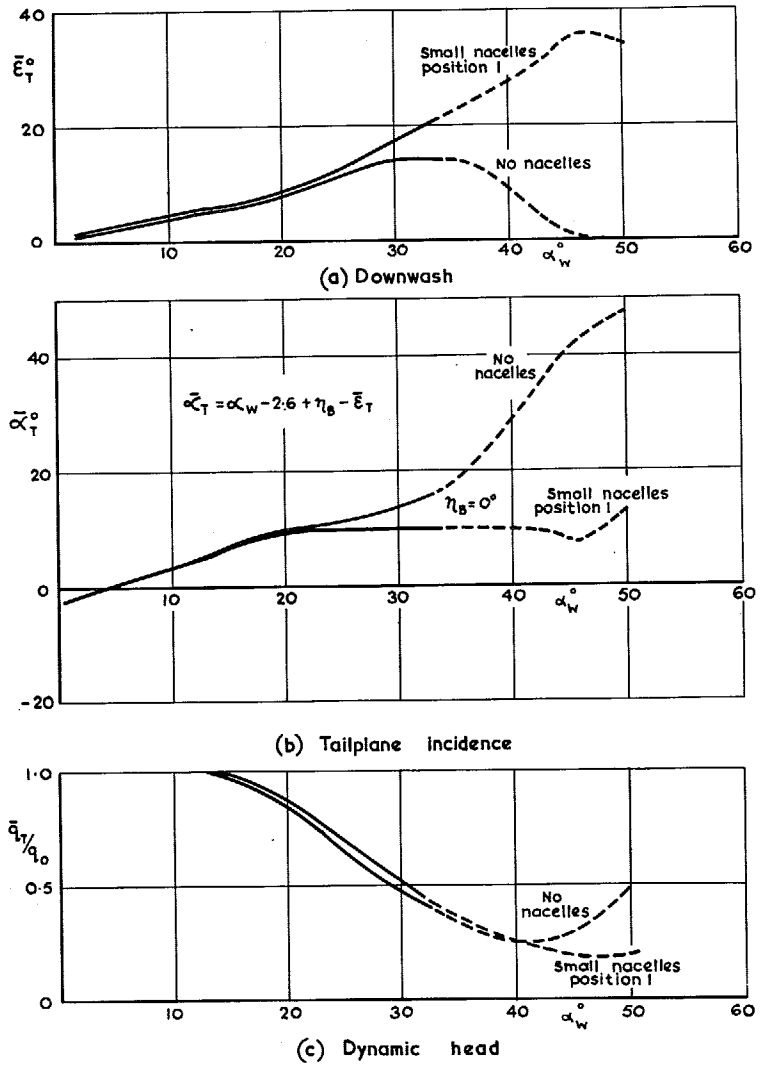

FIG. 36a to c. Mean flow conditions at tailplane position B2. (Derived from pitching moment data with Tailplane 1).

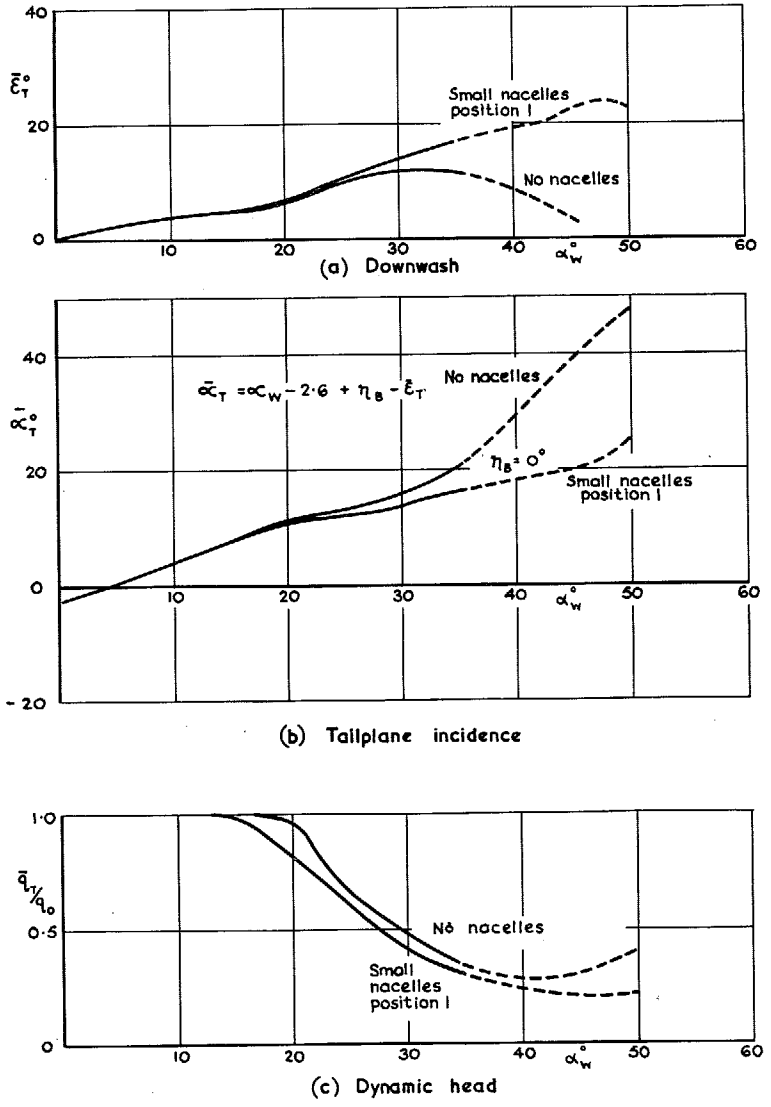

FIG. 37a to c. Mean flow conditions at tailplane position B2. (Derived from pitching moment data with Tailplane 2).

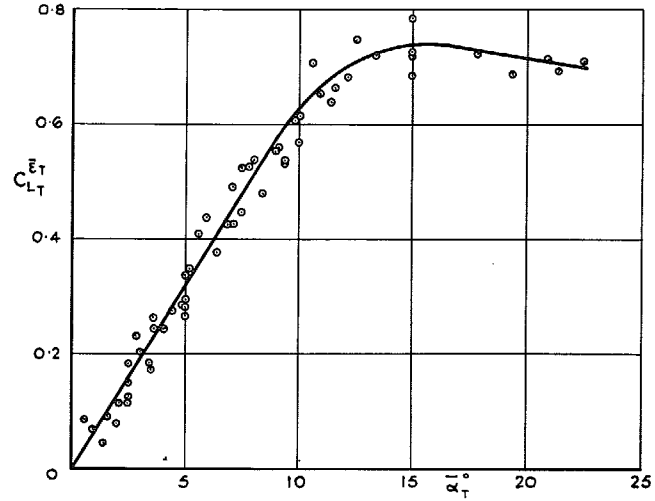

(a) Lift

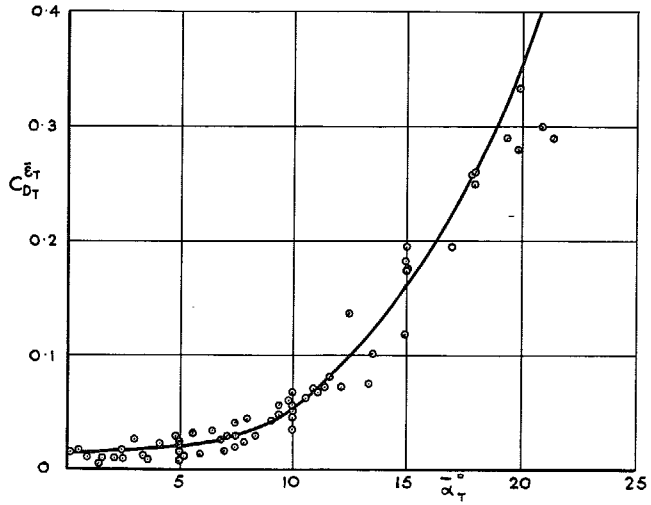

(b) Drag

FIG. 38a and b. Tailplane lift and drag vs. effective incidence. Tailplane 1.

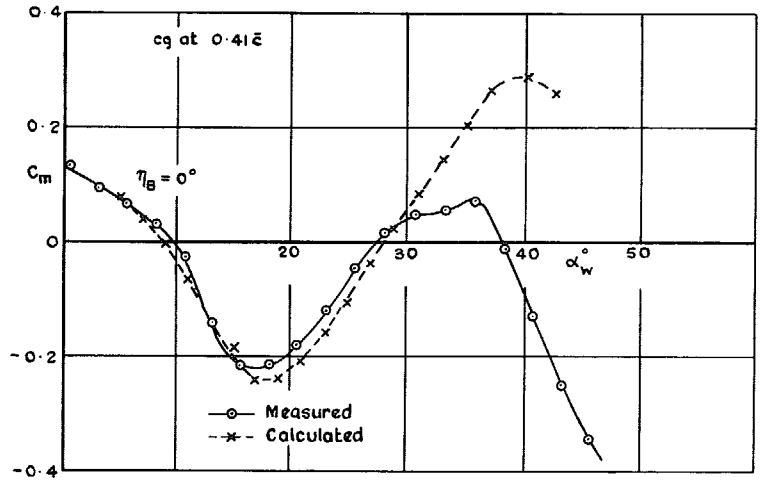

(a) No nacelles

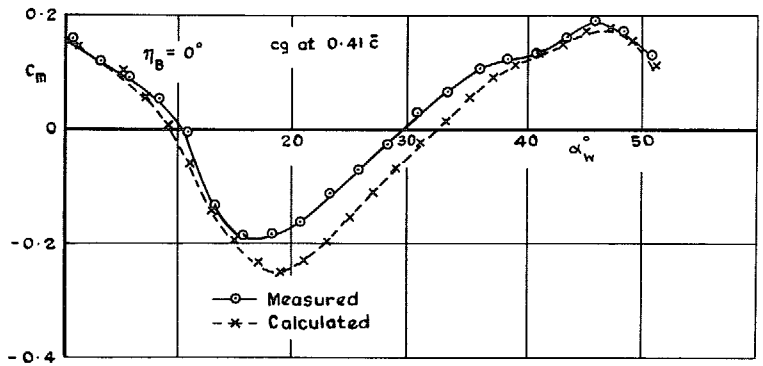

(b) Small nacelles position 1

FIG. 39a and b. Comparison of measured and calculated values of C_m for Tailplane 1 in position B2.

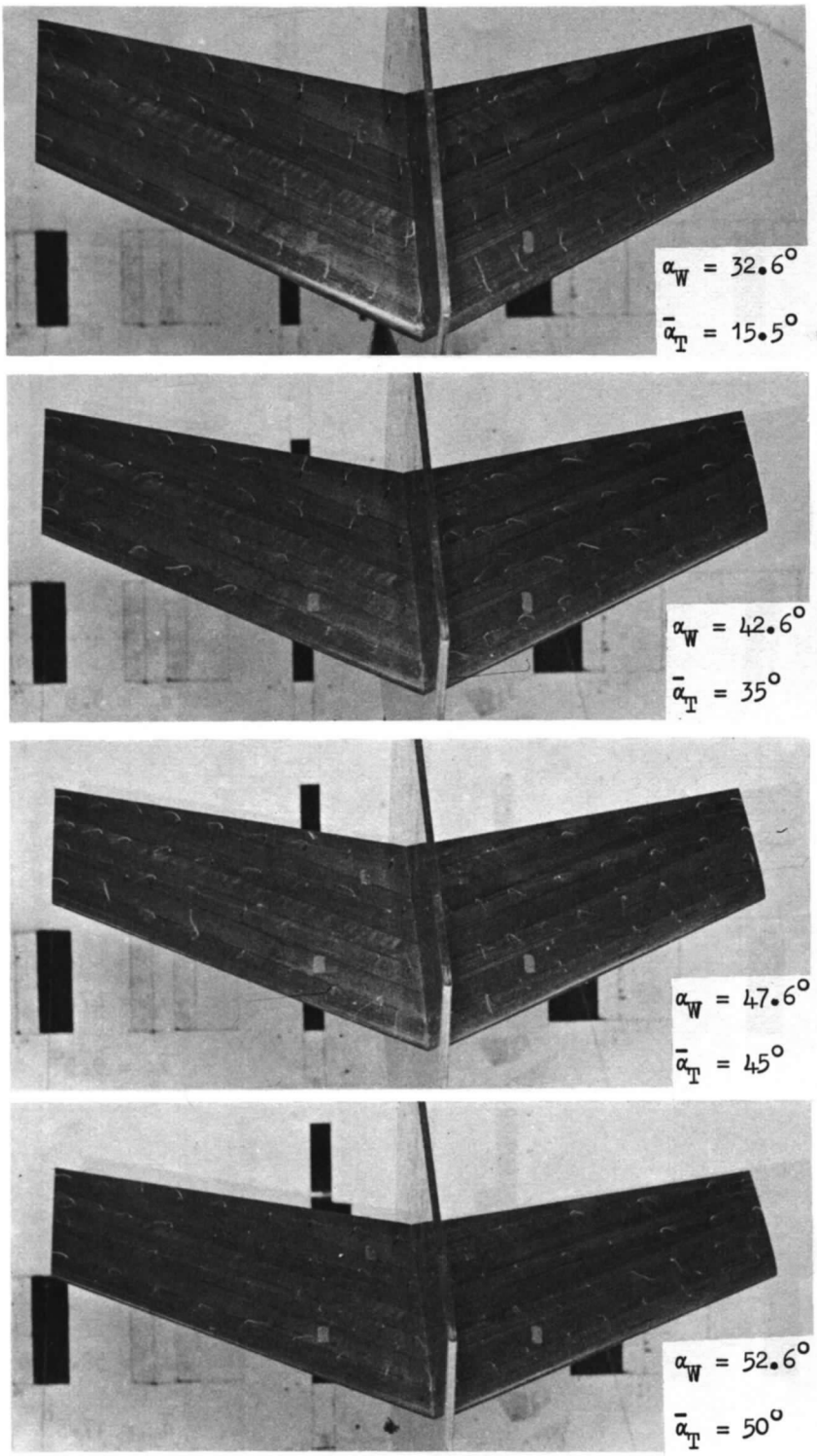

FIG. 40. Tuft patterns on tailplane upper surface. Tailplane 1, position B2, no nacelles, Model 1.

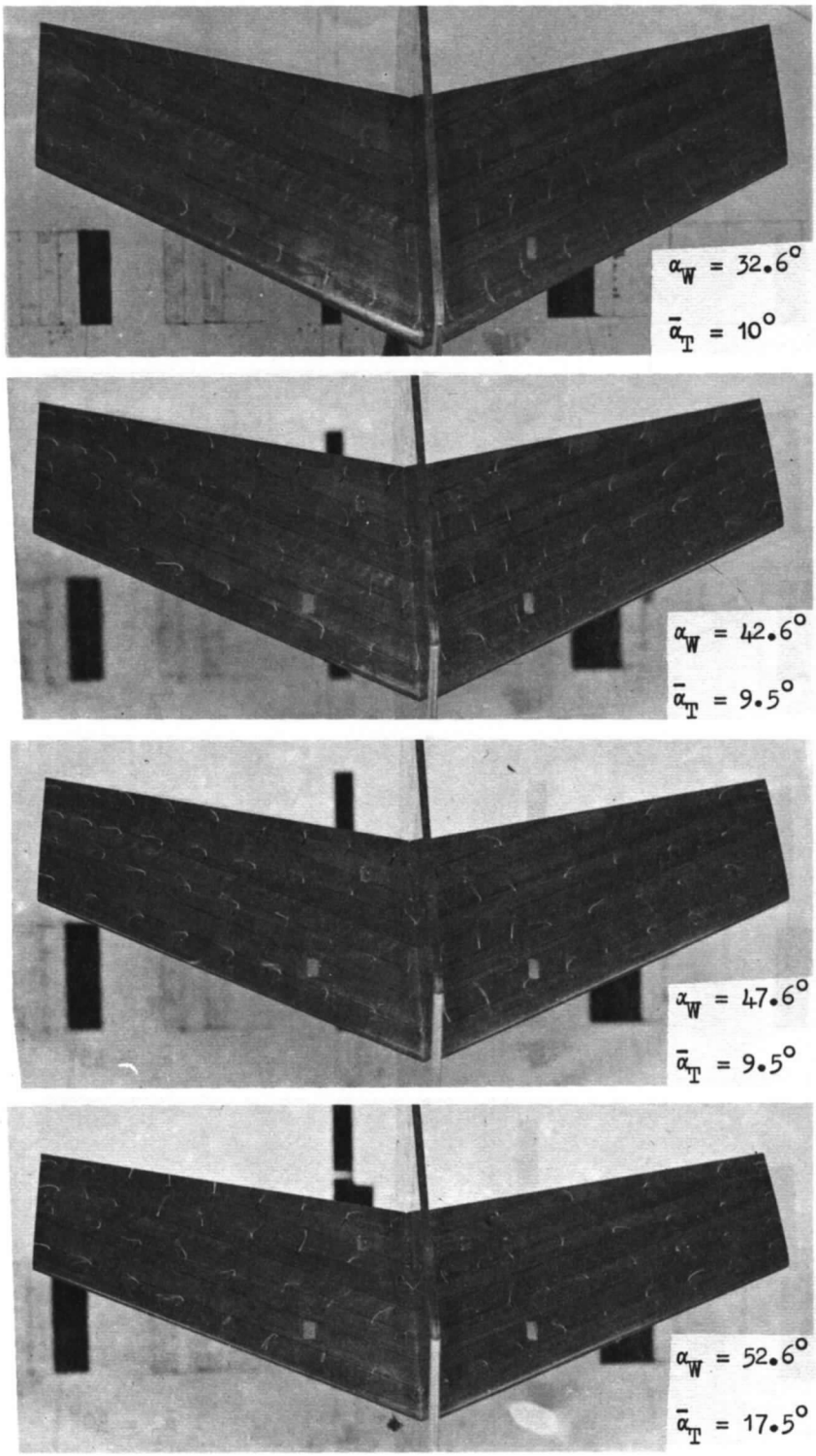

FIG. 41. Tuft patterns on tailplane upper surface. Tailplane 1, position B2, small nacelles, position 1; Model 1.

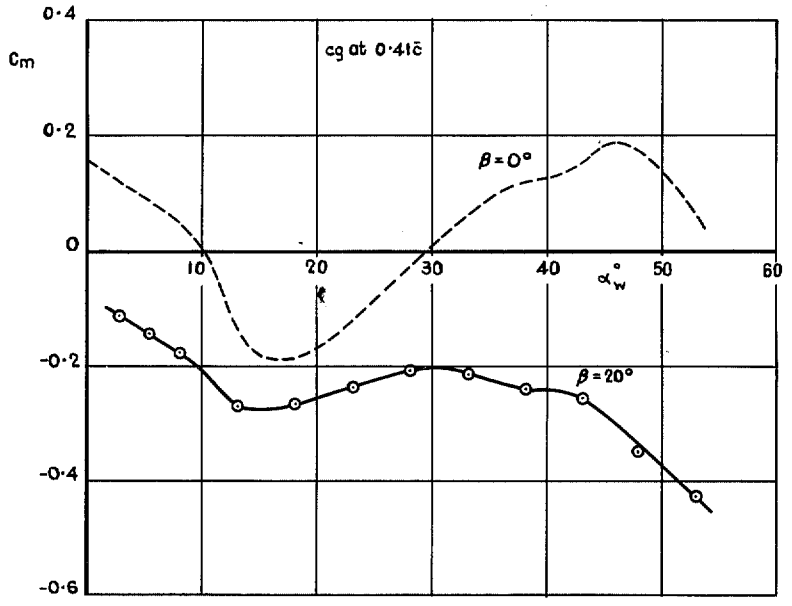

FIG. 42. Effect of sideslip. Model 1, small nacelles, position 1; Tailplane 1, position B2, $\eta_B = 0°$.

Printed in Wales for Her Majesty's Stationery Office by Allens Printers (Wales) Limited

Dd.135646 K.5.

Published by
HER MAJESTY'S STATIONERY OFFICE

To be purchased from
49 High Holborn, London W.C.1
13A Castle Street, Edinburgh 2
109 St. Mary Street, Cardiff CF1 1JW
Brazennose Street, Manchester M60 8AS
50 Fairfax Street, Bristol BS1 3DE
258 Broad Street, Birmingham 1
7 Linenhall Street, Belfast BT2 8AY
or through any bookseller

S.O. Code No. 23-357